# Colorless organometallic ionic liquids from cationic ruthenium sandwich complexes: thermal properties, liquid properties, and crystal structures of [Ru(η(5)-C5H5)(η(6)-C6H5R)][X]…

Komurasaki, Aina
Funasako, Yusuke
Mochida, Tomoyuki

(Citation)
Dalton Transactions,44(16):7595-7605

(Issue Date)
2015-04

(Resource Type)
journal article

(Version)
Accepted Manuscript



(URL)
https://hdl.handle.net/20.500.14094/90002757

# Colorless Organometallic Ionic Liquids from Cationic Ruthenium Sandwich Complexes: Thermal Properties, Liquid Properties, and Crystal Structures of $[Ru(\eta^5\text{-}C_5H_5)(\eta^6\text{-}C_6H_5R)][X]$ ($X = N(SO_2CF_3)_2$, $N(SO_2F)_2$, $PF_6$)

Aina Komurasaki, Yusuke Funasako, and Tomoyuki Mochida*

Department of Chemistry, Graduate School of Science, Kobe University, Rokkodai, Nada, Hyogo 657-8501, Japan.

**Corresponding author E-mail*: tmochida@platinum.kobe-u.ac.jp. Tel/Fax: +81-78-803-5679.

†Electronic supplementary information (ESI) available: DSC charts (Fig. S1), phase transition data (Fig. S2), thermogravimetry data (Fig. S3), and packing diagrams (Fig. S4), crystallographic parameters (Table S1), and viscosity data (Table S2). CCDC-1013743 (for [**1a**][$PF_6$]), -1013744 (for [**2a**][$PF_6$] at 293 K), -1013745 (for [**2a**][$PF_6$] at 100 K), -1013747 (for [**3a**][$PF_6$]), -1013746 (for [**4a**][$PF_6$]), -1013748 (for [**2b**][$PF_6$]), -1013749 (for [**3b**][$PF_6$]). For ESI and crystallographic data in CIF or other electronic format see DOI:

A series of ionic liquids containing cationic ruthenium complexes ($[Ru(C_5H_5)(C_6H_5R)]^+$) were prepared, and their thermal properties were investigated (R = $C_4H_9$ (**1a**), $C_8H_{17}$ (**1b**), $OCH_2OCH_3$ (**2a**), $O(CH_2CH_2O)_2CH_3$ (**2b**), $O(CH_2)_3CN$ (**3a**), $O(CH_2)_6CN$ (**3b**), $CO(CH_2)_2CH_3$ (**4a**), $CO(CH_2)_6CH_3$ (**4b**)). Bis(trifluoromethanesulfonyl)amide (TFSA) and bis(fluorosulfonyl)amide (FSA) were used as counter anions. These ionic liquids were colorless and stable toward air and light. These salts exhibited glass transitions upon cooling from the melt ($T_g$ = –80 °C to –55 °C), and the glass transition temperatures of the salts increased as the polarity of the substituents increased (alkyl < ether < cyano < carbonyl). The decomposition temperatures decreased in the order of alkyl > cyano > carbonyl > ether. The viscosities, solvent polarities, and refractive indices of the salts of **1a** and **2a**

were also evaluated. Hexafluorophosphate ($PF_6$) salts were also prepared, which were solids with high melting points ($T_m$ = 65–130 °C). X-ray crystal structure analyses of these salts revealed the importance of intermolecular contacts involving the ring hydrogens. The $PF_6$ salt of **2a** exhibited an order-disorder phase transition.

## Introduction

Ionic liquids (ILs) are characterized as salts that have melting points below 100 °C. Over recent years, they have attracted much attention because of their characteristic liquid properties.[1] The majority of ionic liquids contain organic cations such as imidazolium, ammonium, and phosphonium cations. Recently, various ILs that feature either metal-containing anions[2] or cations[3,4] have also been developed; these types of compounds exhibit many interesting properties. We have developed metal-containing ILs from sandwich complexes, such as ferrocenium and cobaltocenium cations, and half-sandwich complexes. These organometallic ILs exhibit a variety of magnetic properties[5a–c] and chemical reactivities.[5d–e] However, most of them are intensely colored and are often air- or photo-sensitive.[5a] Air-stable ferrocenium ILs have been reported, but their preparation is tedious.[5b–c] In this study, in order to overcome these drawbacks, we used cationic cyclopentadienyl(arene)ruthenium(II) complexes, which are stable, colorless, and easily prepared.[6]

This paper reports the preparation and properties of ILs containing cyclopentadienyl(arene)ruthenium(II) complexes ($[Ru(\eta^5\text{-}C_5H_5)(\eta^6\text{-}C_6H_5R)]^+$) bearing a series of substituents on the arene ligand, as shown in Fig. 1. Bis(trifluoromethanesulfonyl)amide (TFSA), bis(fluorosulfonyl)amide (FSA), and hexafluorophosphate ($PF_6$) were used as counter anions. The resulting salts were colorless and stable toward light and oxygen. These features are advantageous for both basic investigations and applications. Although only simple alkyl substituents have been used in our studies on organometallic ILs,[5] alkyl, ether, cyano, and carbonyl substituents with variable chain lengths were introduced into the cation in the present study. This variation was

possible because of the use of the ruthenium(II) complexes, allowing systematic investigation of the effects of different substituents on the thermal properties of the IL. Introduction of heteroatoms into the substituents leads to applications such as coordination transformation and ion sensing. Previously, we reported the preparation of $[Ru(\eta^5\text{-}C_5H_5)(\eta^6\text{-}C_6H_4L_2)]X$ (L = $OCH_3$, $N(CH_3)_2$, $SCH_3$; X = $PF_6$, TFSA) complexes, though most of them exhibited high melting points owing to the smaller sizes of the substituents.[7] Furthermore, the colorless nature of the present ILs enabled evaluation of their solvent polarities and refractive indices. The refractive indices of liquids containing heavy atoms are of interest. Crystal structures of the $PF_6$ salts were determined to elucidate cation–anion arrangements and intermolecular interactions.

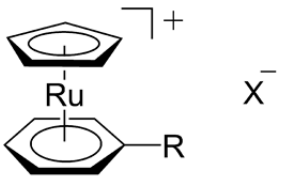


X = TFSA, FSA, $PF_6$

| Cation | R | Cation | R |
|---|---|---|---|
| **1a** | $C_4H_9$ | **1b** | $C_8H_{17}$ |
| **2a** | $OCH_2OCH_3$ | **2b** | $O(CH_2CH_2O)_2CH_3$ |
| **3a** | $O(CH_2)_3CN$ | **3b** | $O(CH_2)_6CN$ |
| **4a** | $CO(CH_2)_2CH_3$ | **4b** | $CO(CH_2)_6CH_3$ |

**Fig. 1** Structural formulae of the ruthenium-containing ionic liquids prepared in this study.

## Results and discussion

### Preparation and properties

$PF_6$ salts were prepared by reacting $[Ru(C_5H_5)(NCCH_3)_3][PF_6]$ with monosubstituted benzenes (yields 92–69%, except for [**3b**][$PF_6$]). The yield of [**3b**][$PF_6$] was exceptionally low (16%) because repeated washing was necessary to remove unreacted ligand. The $PF_6$ salts were solids at room temperature. TFSA salts were prepared from the $PF_6$ salts by metathesis using Li[TFSA] (yields 90–51%). [**2a**][TFSA], [**3a**][TFSA], and [**4b**][TFSA] were solids, while all other salts were liquids. FSA salts were prepared from the $PF_6$ salts using K[FSA] (yields ~60%). [**2a**][FSA], [**3b**][FSA],

[**4a**][FSA], and [**4b**][FSA] were solids, while all other salts were liquids. All of the salts were either colorless or pale yellow, and were stable toward air and visible light. Notably, except for the cyano compounds, the salts were even stable toward UV light. They were soluble in dichloromethane, acetone, and acetonitrile; less soluble in chloroform and ethanol; and not soluble in water, ether, and hexane. The samples were carefully dried under vacuum before the physical properties were measured to remove any traces of solvents or moisture.

**Thermal properties**

The thermal properties of the salts were investigated by differential scanning calorimetry (DSC). The melting points ($T_m$), glass transition temperatures ($T_g$), and relevant thermodynamic parameters of the various salts are listed in Table 1. Their DSC traces are summarized in Fig. S1 in the ESI†.

Except for [**2a**][FSA], which exhibited crystallization upon cooling from the melt, all TFSA and FSA salts exhibited a glass transition upon cooling. The glass transition temperatures of the various salts are plotted in Fig. 2a; $T_g$ increased in the order of **1a/b** < **2a/b** < **3a/b** < **4a/b**. This tendency is consistent with an increase in the polarity of the substituents: alkyl < ether < cyano < carbonyl. The glass transition temperatures of the FSA salts were several degrees lower than those observed for the TFSA salts. Elongation of the substituent (series **a** *vs.* **b**) affected the glass transition temperatures by no more than ±10 °C.

The glass transition temperatures ($T_g$) of the alkyl compounds, TFSA/FSA salts of **1a**–**1b**, were in the –82 °C to –73 °C range, whereas the glass transition temperature of [**1a**][TFSA] ($T_g$ = –74 °C) was higher than that of the ferrocenium-based IL bearing the same substituents ([Fe($C_5H_5$)($C_5H_4{}^nBu$)][TFSA]: $T_g$ = −80.7 °C).[5a] The ether compounds (TFSA/FSA salts of **2a**–**2b**; $T_g$ = –68 °C to –59 °C) exhibited higher glass transition temperatures than did the alkyl compounds, and we observed that the transition temperature increased with elongation of the substituent ([**2a**][TFSA]: $T_g$ = −68 °C *vs.* [**2b**][TFSA]: $T_g$ = −59 °C). These tendencies are probably caused by

the greater polarity of the ether substituents compared to the alkyl substituents. In imidazolium ILs, the introduction of an ether moiety into the cation often lowers the melting points owing to increased flexibility, but the melting points also increase in some cases.[8,9] The cyano compounds (TFSA/FSA salts of **3a**–**3b**; $T_g$ = −63 °C to −56 °C) also exhibited higher glass transition temperatures than did the alkyl compounds. Indeed, in onium ILs, the introduction of a cyano group to the cation has been reported to increase intermolecular interactions, resulting in an increase in the melting point and glass transition temperature.[10,11] The carbonyl compounds (TFSA/FSA salts of **4a**–**4b**; $T_g$ = −58 °C to −55 °C) exhibited the highest glass transition temperatures, and all salts, except for [**4a**][TFSA], were obtained as crystals at room temperature.

The melting points of the TFSA and FSA salts that were obtained as crystals were in the 30.8–70.4 °C range. These salts followed the empirical relationship $T_g/T_m$ = 2/3,[12] which generally holds for molecular liquids (Table 1). The melting entropies of these salts were higher than 50 J $K^{-1}$ $mol^{-1}$, and only [**4a**][FSA] exhibited a phase transition in the solid state. The phase transition data, including those of the $PF_6$ salts, are summarized in Table 2. The melting points and glass transition temperatures of the TFSA salts were lower than those of [Ru($\eta^5$-$C_5H_5$)($\eta^6$-$C_6H_4L_2$)]TFSA (L = $OCH_3$, $N(CH_3)_2$, $SCH_3$) complexes bearing short substituents ($T_m$ = 54.1–60.8 °C; $T_g$ = −62 °C to −38 °C).[7]

The $PF_6$ salts were solids with high melting points ($T_m$ = 65–130 °C, Fig. 2b), with only three exhibiting glass transitions when cooled from the melt. Their melting points were lower than those of [Ru($\eta^5$-$C_5H_5$)($\eta^6$-$C_6H_4L_2$)]$PF_6$ (L = $OCH_3$, $N(CH_3)_2$, $SCH_3$) complexes ($T_m$ = 150–200 °C).[7] The melting points of the short-chain compounds (Series **a**) with higher-polarity substituents were found to be higher. This was observed in the order of alkyl < ether < cyano < carbonyl. Lengthening the substituents, moving from Series **a** to Series **b,** resulted in a remarkable decrease in the melting points of the various salts by as much as 40–60 °C. The only exception was in the case of the alkyl compounds, and hence, the effect of elongating the substituent was much larger in the $PF_6$ salts than

in the TFSA and FSA salts. The $T_g/T_m$ values for the $PF_6$ salts (0.68–0.72) were slightly higher than 2/3. Interestingly, the melting entropies of [**1a**][$PF_6$] ($\Delta S_m$ = 22.8 J $K^{-1}$ $mol^{-1}$) and [**1b**][$PF_6$] ($\Delta S_m$ = 20.8 J $K^{-1}$ $mol^{-1}$) were particularly low, suggesting that their high-temperature phases are accompanied by extensive orientational disorder.[13] All $PF_6$ salts, with the exception of [**3a**][$PF_6$], [**3b**][$PF_6$], and [**4b**][$PF_6$], exhibited phase transitions in the solid state (Table 2), and [**1b**][$PF_6$] exhibited a glass transition ($T_g$ = –20 °C) in the crystal phase, likely resulting from the freezing of the motion of the alkyl substituent at lower temperatures. No clear correlation was observed between the total phase transition entropies (Fig. S2 in the ESI†) and the cation species.

**Table 1** Glass transition temperatures ($T_g$), melting points ($T_m$), melting enthalpies ($\Delta H_m$), and melting entropies ($\Delta S_m$)

| | $T_g$ (°C) | $T_m$ (°C) | $\Delta H_m$ (kJ $mol^{-1}$) | $\Delta S_m$ (J $K^{-1}$ $mol^{-1}$) | $T_g/T_m$ |
|---|---|---|---|---|---|
| TFSA salts | | | | | |
| [**1a**][TFSA] | –74 | | | | |
| [**1b**][TFSA] | –73 | | | | |
| [**2a**][TFSA] | –68 | 30.8 | 31.2 | 101.4 | 0.67 |
| [**2b**][TFSA] | –59 | | | | |
| [**3a**][TFSA] | –56 | 69.5 | 37.7 | 108.9 | 0.63 |
| [**3b**][TFSA] | –63 | | | | |
| [**4a**][TFSA] | –55 | | | | |
| [**4b**][TFSA] | –57 | 70.4 | 34.8 | 100.7 | 0.63 |
| FSA salts | | | | | |
| [**1a**][FSA] | –82 | | | | |
| [**1b**][FSA] | –76 | | | | |
| [**2a**][FSA] | | 33.5 | 22.0 | 70.3 | |
| [**2b**][FSA] | –61 | | | | |
| [**3a**][FSA] | –60 | | | | |
| [**3b**][FSA] | –62 | 43.5 | 33.2 | 104.9 | 0.67 |
| [**4a**][FSA] | –56 | 64.6 | 19.1 | 56.4 | 0.64 |
| [**4b**][FSA] | –58 | 49.8 | 49.0 | 150.4 | 0.67 |

| | | | | | |
|---|---|---|---|---|---|
| **$PF_6$ salts** | | | | | |
| [**1a**][$PF_6$] | | 87.0 | 7.8 | 22.8 | |
| [**1b**][$PF_6$] | | 85.8 | 7.6 | 20.8 | |
| [**2a**][$PF_6$] | | 109.1 | 18.2 | 47.5 | |
| [**2b**][$PF_6$] | –36 | 70.3 | 22.8[a] | 67.3[a] | 0.69 |
| [**3a**][$PF_6$] | | 114.9 | 32.3 | 83.1 | |
| [**3b**][$PF_6$] | –41 | 66.3 | 32.3 | 94.5 | 0.68 |
| [**4a**][$PF_6$] | | 127.2 | 16.0[a] | 39.8[a] | |
| [**4b**][$PF_6$] | –29 | 65.1 | 10.5[a] | 30.5[a] | 0.72 |

[a] Including the contribution of a solid phase transition occurring prior to melting.

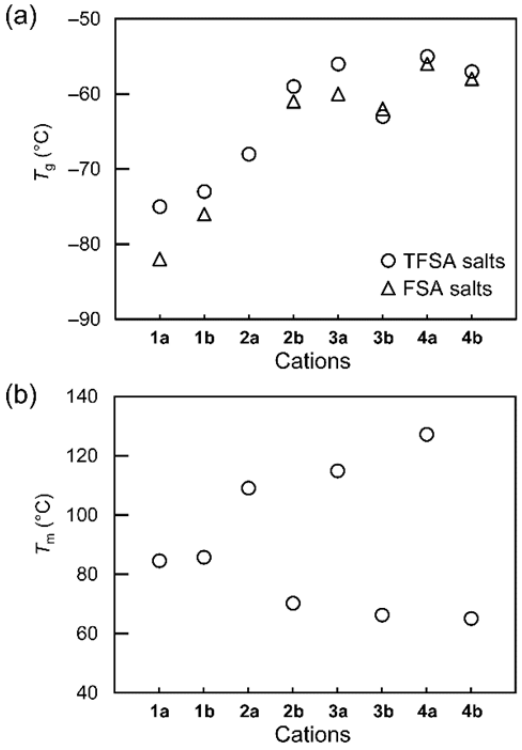


**Fig. 2** (a) Glass transition temperatures ($T_g$) of the TFSA and FSA salts. (b) Melting points ($T_m$) of the $PF_6$ salts.

**Table 2** Data for phase transitions in the solid state. Phase transition temperatures ($T_c$), enthalpies ($\Delta H_c$) and entropies ($\Delta S_c$) of phase transition.

| | $T_c$ (°C) | $\Delta H$ (kJ mol$^{-1}$) | $\Delta S$ (J K$^{-1}$ mol$^{-1}$) |
|---|---|---|---|
| [**4a**][FSA] | –98.1 | 1.4 | 7.9 |
| [**1a**][$PF_6$] | 62.8 | 8.7 | 26.3 |
| | 73.0 | 5.6 | 16.6 |
| [**1b**][$PF_6$] | 54.7 | 2.1 | 6.5 |
| [**2a**][$PF_6$] | –89.0 | 0.2 | 1.0 |
| [**2b**][$PF_6$] | 44.8 | 5.7 | 18.0 |
| | 62.4 | 22.8[a] | 67.3[a] |
| [**4a**][$PF_6$] | 121.9 | 16.0[a] | 39.8[a] |
| | 51.0[b] | 0.3[b] | 0.9[b] |

[a] The value includes that of melting occurring after the phase transition. [b] Observed after the second cycle.

**Thermal stability**

The thermal stabilities of the TFSA and FSA salts were investigated by thermogravimetric (TG) analysis. The decomposition temperatures ($T_{dec}$) are given in Table 3 (at 3% weight loss, 10 K min$^{-1}$), and the TG traces are shown in Fig. S3 in the ESI†. We observed that the decomposition temperatures of the TFSA salts decreased in the order of [**1a**][TFSA] ($T_{dec}$ = 377 °C) > [**3a**][TFSA] (345 °C) > [**4a**][TFSA] (337 °C) > [**2a**][TFSA] (279 °C), indicating the relative stability of the cations as follows: alkyl > cyano > carbonyl > ether. The decomposition temperature of [**1a**][TFSA] was higher than those of ferrocenium ILs[5a] (e.g., [Fe($C_5H_4Et)_2$][TFSA]: $T_{dec}$ = 188 °C (1 K min$^{-1}$); [Fe($C_5Me_4C_6H_{13}$)($C_5Me_4H$)][TFSA]: $T_{dec}$ = 342 °C; and [Fe($C_5H_5$)($C_6H_4Et$)][TFSA]: $T_{dec}$ = 218 °C (1 K min$^{-1}$)). These data indicate that Ru-containing ILs exhibit higher thermal stability than do their Fe-containing analogs. However, it was also observed that the Ru-containing ILs were less stable than the cobaltocenium ILs (e.g., [Co($C_5H_4Et)_2$][TFSA]: $T_{dec}$ = 413 °C)[5a] and the alkylimidazolium

ILs (e.g., 1-butyl-3-methylimidazolium TFSA: $T_{dec}$ = 423 °C).[14] The introduction of a cyano group into the imidazolium cation lowers the $T_{dec}$ by approximately 40 °C (e.g., 1-butyronitrile-3-methylimidazolium TFSA: $T_{dec}$ = 384 °C (−5%wt)[9]). Similarly, the decomposition temperature of cyano compound [**3a**][TFSA] was lower than that of [**1a**][TFSA] by approximately 30 °C. The ether compound [**2a**][TFSA] exhibited the lowest stability, although cyclopentadienyl(arene)ruthenium(II) complexes with electron-donating substituents are expected to be more thermally stable than those without.[7,15] This lower stability is likely due to dissociation of the ether group. This is supported by the observation of two-step thermal decomposition in ether compounds ([**2a**][TFSA] and [**2a**][FSA]), where the dissociation accounts for the weight loss in the first step. The introduction of an ether substituent into the imidazolium cation also lowers the thermal stability of the ILs.[8]

The FSA salts were much less thermally stable than the TFSA salts were, as often observed in other ILs.[16,17] This could be attributed to the lower thermal stability of the anion toward pyrolysis.[18] The decomposition temperatures of the FSA salts were in the 241–265 °C range. The order of their thermal stabilities was comparable to that observed for the TFSA salts, although in the case of the FSA salts, the relative differences in the decomposition temperatures were much lower.

**Table 3** Decomposition temperatures determined by TG analysis (at −3%wt, 10 K min$^{-1}$)

| | $T_{dec}$ (°C) | | $T_{dec}$ (°C) |
|---|---|---|---|
| [**1a**][TFSA] | 377 | [**1a**][FSA] | 265 |
| [**2a**][TFSA] | 279 | [**2a**][FSA] | 241 |
| [**3a**][TFSA] | 345 | [**3a**][FSA] | 253 |
| [**4a**][TFSA] | 337 | [**4a**][FSA] | 247 |

**Liquid properties**

Viscosities, refractive indices, and solvent polarity parameters of [**1a**][TFSA], [**1a**][FSA], and [**2a**][FSA] were evaluated as representative examples.

Temperature dependence of the viscosities of the liquids is shown in Fig. 3. The viscosity data and relevant parameters are summarized in Table 4. The viscosity of [**1a**][TFSA] (136.6 mPa s, at 25 °C) was comparable to that of the corresponding ferrocenium IL, [Fe($C_5H_5$)($C_5H_4{}^n$Bu)][TFSA] (112.3 mPa s).[5a] The viscosity of [**1a**][FSA] (90.8 mPa s) was lower than that of [**1a**][TFSA], which is consistent with the tendency of FSA to give low-viscosity ILs.[19] The viscosity of [**2a**][FSA] (338.4 mPa s) was three times higher than that of [**1a**][FSA]. This is probably ascribed to the higher polarity of the ether group on **2a** compared to the alkyl group on **1a**. These ILs were more viscous than the typical imidazolium ILs (e.g., [bmim][TFSA]: 49 mPa s, bmim = 1-butyl-3-methylimidazolium).[20a] The activation energies ($E_a$) determined from the Arrhenius plots ($\eta = \eta_0 e^{Ea/RT}$) were 30–40 kJ mol$^{-1}$ (Table 4), which are comparable to that of [bmim][TFSA] (31.3 kJ mol$^{-1}$).[20] The Vogel-Tammann-Fulcher (VTF) equation ($\eta = \eta_0 \exp[DT_0/(T-T_0)]$)[21] was also used to fit the data (Table 4), where $T_0$ is the ideal glass transition temperature and $D$ is a parameter that shows deviation from Arrhenius behavior. The small $D$ values (3.4–6.5), which are comparable to that of [bmim][TFSA] ($D$ = 4.65),[20] suggest that they are fragile liquids.[22] It is reasonable that the viscosity data for [**1a**][TFSA] are similar to those for the corresponding ferrocenium IL, [Fe($C_5H_5$)($C_5H_4{}^n$Bu)][TFSA].

The refractive indices of [**1a**][TFSA], [**1a**][FSA], and [**2a**][FSA] at 20 °C were 1.509, 1.540, and 1.546, respectively. This increase can be associated with the increase in density in the order of [**1a**][TFSA], [**1a**][FSA], and [**2a**][FSA]. The refractive indices of [**1a**][FSA] at 20 °C, 30 °C, and 40 °C were 1.540, 1.537, and 1.534, respectively; this inverse relationship between temperature and refractive index was ascribed to thermal expansion. The values, which are similar to those of other ruthenium complexes,[23,24] are relatively low despite the fact that these complexes each possess a heavy atom at their center.

The solvent polarity parameters ($E_T{}^N$) of both [**1a**][TFSA] and [**1a**][FSA] were found to be 0.51 at 20 °C. The $E_T{}^N$ values for [**2a**][FSA] measured at 30 °C and 40 °C were equal (0.54), and the

solvent polarity parameter at 20 °C could not be obtained due to crystallization. The higher value obtained for [**2a**][FSA] is likely due to the polarity of the ether substituent. The values obtained for these liquids are comparable to those of cobaltocenium salt $[Co(C_5H_4Et)_2][TFSA]$ ($E_T^N = 0.54$)[5a] and cyclohexanol ($E_T^N = 0.509$),[25] but lower than those of typical imidazolium ionic liquids ($E_T^N = 0.6$–0.7).[26]

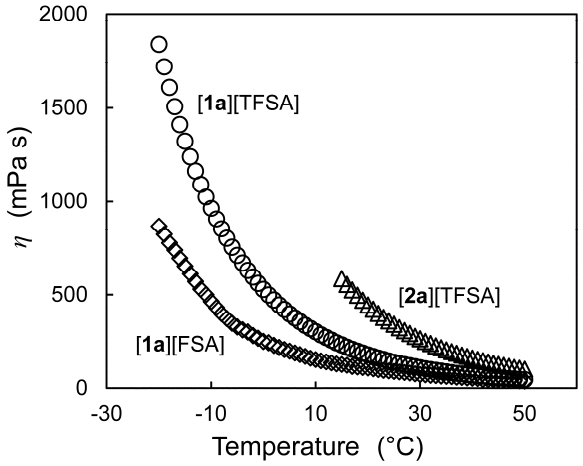


**Fig. 3.** Temperature dependence of the viscosities of [**1a**][TFSA], [**1a**][FSA], and [**2a**][FSA].

**Table 4** Viscosities and relevant parameters

| | $\eta_{25\,°C}$ (mPa s) | $E_a$ (kJ mol$^{-1}$) | $D$ value | $\eta_0$ (mPa s) | $T_0$ (°C) |
|---|---|---|---|---|---|
| [**1a**][TFSA] | 136.6 | 35.8 | 5.6 | 0.22 | –115.2 |
| [**1a**][FSA] | 90.8 | 29.8 | 6.5 | 0.21 | –130.8 |
| [**2a**][FSA] | 338.4 | 38.4 | 3.4 | 0.76 | –82.1 |
| $[Fe(C_5H_5)(C_5H_4{}^nBu)][TFSA]$[a] | 112.3 | 38.8 | 4.6[c] | 0.33[c] | –106.8[c] |
| [bmim][TFSA][b,d] | 49 | 31.3 | 4.7 | 0.25 | –108.5 |

[a] Ref. 5a. [b] Ref. 20. [c] Revised values. [d] bmim = 1-butyl-3-methylimidazolium cation.

### Crystal structures of $PF_6$ salts

Crystal structures of [**1a**][$PF_6$], [**2a**][$PF_6$], [**2b**][$PF_6$], [**3a**][$PF_6$], [**3b**][$PF_6$], and [**4a**][$PF_6$] were determined by X-ray crystallography at −173 °C. The structure of [**2a**][$PF_6$] was also determined at 20 °C to elucidate the nature of the phase transition at −89.0 °C. The structures of the cations present in these salts are given in Figs. 4 and 5. As can be seen in Figs. 4b and 5b, the alkyl substituents are generally oriented in a linear manner, whereas the ether moieties on **2a** and **2b** exhibit bent structures.

The alkyl-cyano substituent on **3a** appears more twisted than the other structures obtained. The carbonyl group in **4a** was nearly coplanar with the benzene ring. The anions in [**2a**][$PF_6$] (at 20 °C), [**3a**][$PF_6$], and [**3b**][$PF_6$] were disordered.

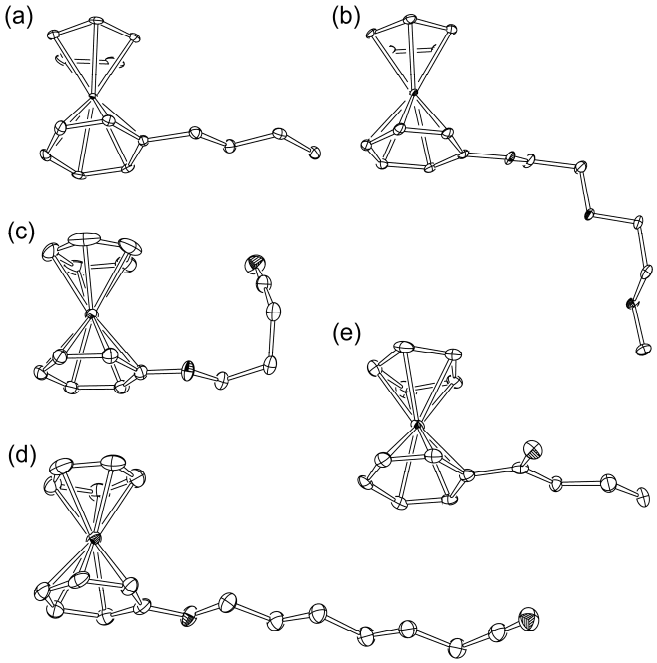


**Fig. 4** The structures of cations in (a) [**1a**][$PF_6$], (b) [**2b**][$PF_6$], (c) [**3a**][$PF_6$], (d) [**3b**][$PF_6$], and (e) [**4a**][$PF_6$] at −173 °C (50% thermal probability ellipsoids).

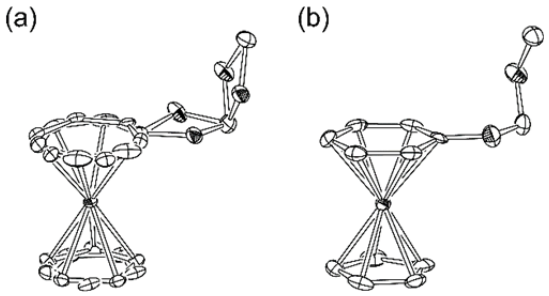


**Fig. 5** The molecular structures of cations in [**2a**][$PF_6$] at (a) 20 °C (20% thermal probability ellipsoids) and (b) −173 °C (50% thermal probability ellipsoids).

The cations and anions were arranged alternately in these salts, and no layered structures were

formed. The packing diagrams of [**1a**][$PF_6$], [**3b**][$PF_6$], and [**2a**][$PF_6$] are shown in Figs. 6 and 7, and those of the other salts can be found in Fig. S4 in the ESI†. The anions are located near the cationic sandwich moieties (Fig. 6), and hence, many short contacts between the ring hydrogens and the anions were found in the structure. All salts, with the exception of [**1a**][$PF_6$], exhibited short intermolecular contacts between the benzene hydrogens and the fluorine atoms (CH···F: 2.24–2.36 Å). The distances are shorter than the typical van der Waals (vdW) contact distances by approximately 0.3 Å, and they are regarded as weak hydrogen bonds. Also observed were contacts between the cyclopentadienyl hydrogens and the fluorine atoms (CH···F: 2.24–2.50 Å), which are shorter than the vdW distances by 0.1–0.3 Å. Intermolecular π–π contacts between the cations existed only in [**2b**][$PF_6$] and were identified by the presence of C···C contacts between adjacent benzene rings (3.19 Å), which are shorter than the vdW distances by 0.2 Å. There were no notable interactions between the alkyl chains except in [**3b**][$PF_6$], where the chains arranged themselves in close proximity to each other (Fig. 6b). These structural features demonstrate the importance of the ring hydrogen atoms in the formation of these assembled structures. Further supporting this is the observation that salts containing a polymethylated ferrocenium cation such as [$Fe(C_5Me_4H)(C_5Me_4R)$][$PF_6$] (R = $C_6H_{13}$, $C_{10}H_{21}$), which possess only one ring hydrogen atom, give layered structures in the solid state, which is in contrast to the salts discussed above.[5c] In the crystals of 1-alkyl-3-methylimidazolium salts, cation–anion contacts involving the acidic hydrogen at the 2-position have been observed, and their importance on the assembled structures have been discussed.[27]

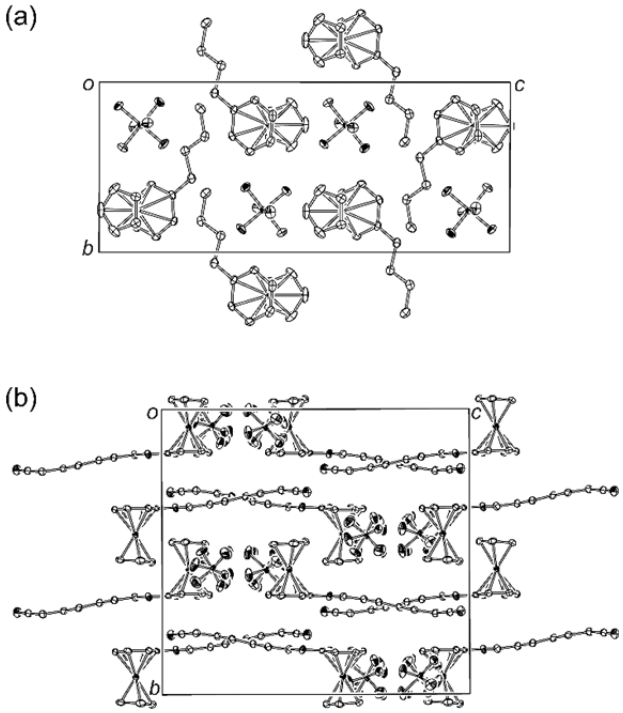


**Fig. 6** Packing diagrams of (a) [**1a**][$PF_6$] and (b) [**3b**][$PF_6$] at −173 °C.

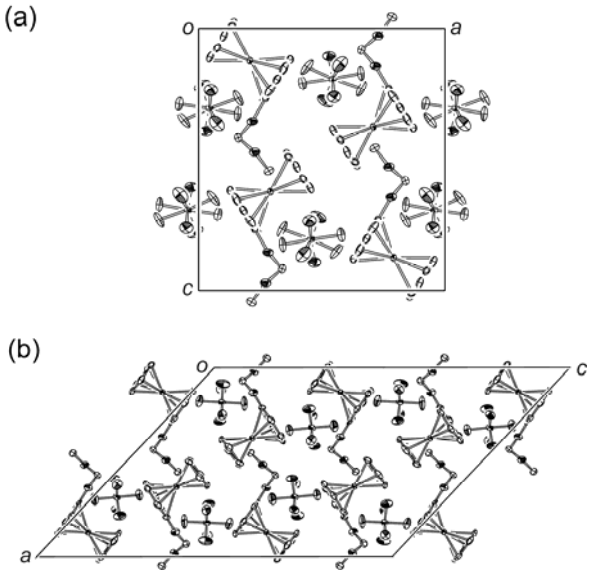


**Fig. 7** Packing diagrams of [**2a**][$PF_6$] at (a) 20 °C and (b) −173 °C.

In addition to the interactions discussed above, compounds with substituents containing heteroatoms exhibited short intermolecular contacts between the heteroatoms and hydrogen atoms. Compounds bearing an ether moiety displayed CH···O interactions between the terminal oxygen

atoms of the substituent and the ring hydrogens (e.g., [**2a**][$PF_6$]: 2.58 and 2.59 Å, [**2b**][$PF_6$]: 2.32 and 2.51 Å), which are shorter than typical vdW distances by 0.3–0.1 Å. Compounds bearing a cyano moiety displayed $C_{Ar}H\cdots NC$ contacts ([**3a**][$PF_6$]: 2.52 Å, [**3b**][$PF_6$]: 2.47 Å), which are shorter than the vdW distances by 0.2 Å. [**4a**][$PF_6$] exhibited short intermolecular contacts between the benzene hydrogen and carbonyl oxygen (CH···O: 2.41 Å), which were 0.3 Å shorter than the vdW distance. It is likely that such weak hydrogen-bond-like intermolecular interactions also exist in the TFSA and FSA salts, thus providing a rationale for their increased melting points and viscosities.

The crystal structures of [**2a**][$PF_6$] were determined above and below the phase transition temperature ($T_C$ = −89.0 °C). Phase transitions in metallocenium salts have received much attention over the years.[28] The packing diagrams are shown in Fig. 7. The phase transition was found to accompany order-disorder of the molecules and cell-doubling ($V$ = 1567 Å$^3$ and Z = 4 (20 °C); $V$ = 2973 Å$^3$ and $Z$ = 8 (−173 °C)), and the space group changed from $P$nma (20 °C) to $P2_1/c$ (−173 °C). The density of the salt changed from 1.908 g cm$^{-3}$ (20 °C) to 2.007 g cm$^{-3}$ (−173 °C), and the increase is comparable to those in other salts exhibiting order-disorder phase transitions.[28a] This salt contains one crystallographically independent pair of cation and anion at room temperature, which are both disordered. The cation is located on the mirror plane, and both the cyclopentadienyl and benzene rings of the cation exhibit two-fold disorder, along with disorder of the substituent moiety (Fig. 5a). In the low-temperature phase, however, the cation and anion are ordered (Fig. 5b), with the number of crystallographically independent molecules doubling and the two crystallographically independent cations exhibiting comparable structures. Interestingly, although the phase transition in this salt accompanies an order-disorder phenomenon, the phase transition entropy was actually very low (0.2 J K$^{-1}$ mol$^{-1}$). This is envisaged to be due to the difference in the lattice entropy of the system compensating for the entropy change of the order-disorder transformation.

## Conclusions

A series of organometallic ILs were prepared from ruthenium(II) complexes $[Ru(\eta^5\text{-}C_5H_5)(\eta^6\text{-}C_6H_5R)]^+$ bearing monosubstituted benzene ligands. Although the cations previously employed for the preparation of metallocenium ILs were generally intensely colored and often air- or photo-sensitive, the ILs prepared in this study were colorless and stable toward light, heat, and oxygen. Their stability and ease of preparation enabled systematic investigation of the effects of substituents on their thermal properties; introduction of heteroatoms in the substituent was found to raise the glass transition temperatures and melting points to some extent. The colorless feature enabled investigation of solvent polarity and refractive indices. The structure-property relationships revealed in the current study are useful for the design of organometallic ILs. The effects of the position of the substituents will also be reported in a subsequent paper.[5f] Investigations on the photochemical reactivities and electrochemical properties of these and relevant ILs are underway in our laboratory.

## Experimental section

### General

$[Ru(C_5H_5)(NCCH_3)_3][PF_6]$,[6b] (methoxymethoxy)benzene,[29] and 2-(2-methoxyethoxy)ethoxybenzene[30] were prepared according to literature methods. Other chemicals were commercially available. $^1$H NMR spectra were recorded on either a JEOL JNM-ECL-400 spectrometer or a Bruker Avance 500 spectrometer. Elemental analyses were carried out either on a Yanaco CHN MT5 analyzer or a PerkinElmer 2400II elemental analyzer. DSC measurements were performed using a TA Q100 differential scanning calorimeter at a scan rate of 10 K min$^{-1}$. Thermogravimetric analyses were performed at a heating rate of 10 K min$^{-1}$ under a nitrogen atmosphere using a Rigaku TG 8120 thermal analyzer. IR spectra were acquired *via* attenuated total reflectance (ATR) using a Thermo Scientific Nicolet iS5 spectrometer. UV spectra

were recorded on a JASCO V-570 UV/VIS/NIR spectrometer. Mass spectra were obtained by positive ion electrospray (ES+) using LTQ Orbitrap Discovery (Thermo Fisher Scientific). Viscosities were measured with a Toki Sangyo TV-22L viscometer using a 3 R7.7 cone rotor. Refractive indices of the liquids were recorded on Anton Paar Abbemat 550 (589 nm, Na-D). Solvent polarities of the ionic liquids were evaluated using the maximum absorption wavelength ($\lambda_{max}$) of the dyes dissolved in the ionic liquids. $E_T^N$ values were determined from the following equations using Reichardt's dye: $E_T^N = [E_T(30) - 30.7]/32.4$, $E_T(30) = 28591/\lambda_{max}$ (nm).[25]

**Preparation of ligands**

**4-Phenoxybutyronitrile.** Under a nitrogen atmosphere, phenol (0.49 g, 5.2 mmol), 4-bromobutanenitrile (0.5 mL, 5.0 mmol), potassium carbonate (5.0 g, 36.0 mmol), potassium iodide (0.33 g, 2.0 mmol), and 18-crown-6-ether (87.0 mg, 0.30 mmol) were dissolved in DMF (20 mL), and the mixture heated at 90 °C for 41 h with stirring. After cooling, a mixture of ethyl acetate and hexane (50 mL, 1:1 v/v) was added, and mixture filtered. The filtrate was washed with brine, dried over $MgSO_4$, and the solvent evaporated under reduced pressure. The residue was dissolved in toluene and purified by column chromatography (silica gel, eluent: toluene/dichloromethane, gradient from 1:0 to 0:1). The solution was evaporated under reduced pressure and the residue dried under vacuum at room temperature for 3 days. The desired product was isolated as a white solid (0.38 g, Yield 58%). $^1$H NMR (400 MHz, $CDCl_3$): δ = 2.15 (quint, 2H, $J$ = 6.5 Hz, C$H_2$CN), 2.60 (t, 2H, $J$ = 7.0 Hz, C$H_2$C$H_2$CN), 4.08 (t, 2H, $J$ = 5.8 Hz, C$H_2$C$_2$H$_4$CN), 6.90 (d, 2H, $J$ = 8.4 Hz, Ar–$H_2$), 6.98 (t, 1H, $J$ = 7.4 Hz, Ar–$H$), 7.30 (t, 2H, $J$ = 7.1 Hz, Ar–$H_2$).

**7-Phenoxyheptanenitrile.** Preparation as described for 4-phenoxybutyronitrile, using phenol (0.73 g, 7.76 mmol), 7-bromoheptanenitrile (1.53 g, 8.07 mmol), potassium carbonate (7.5 g, 54.3 mmol), potassium iodide (0.50 g, 3.01 mmol), and 18-crown-6-ether (0.13 g, 0.49 mmol). The desired product was obtained as a colorless liquid (0.98 g, Yield 62%). $^1$H NMR (400 MHz,

acetone-$d_6$): δ = 1.51 (m, 4H, (C$H_2$)$_2$CN), 1.68 (m, 2H, C$H_2$C$_2$H$_4$CN), 1.79 (m, 2H, C$H_2$C$_3$H$_6$CN), 2.34 (t, 2H, $J$ = 7.0 Hz, C$H_2$C$_4$H$_8$CN), 3.95 (t, 2H, $J$ = 6.2 Hz, C$H_2$C$_5$H$_{10}$CN), 6.89 (d, 2H, $J$ = 8.4 Hz, Ar–$H_2$), 6.93 (t, 1H, $J$ = 7.4 Hz, Ar–$H$), 7.28 (t, 2H, $J$ = 8.0 Hz, Ar–$H_2$).

**Synthesis of [Ru(C$_5$H$_5$)(C$_6$H$_5$C$_4$H$_9$)][X] ([1a][X]; X = PF$_6$, TFSA, FSA)**

**[1a][PF$_6$].** Under a nitrogen atmosphere, *n*-butylbenzene (70 μL, 0.45 mmol) was added to a solution of [Ru(C$_5$H$_5$)(NCCH$_3$)$_3$][PF$_6$] (87.0 mg, 0.20 mmol) in acetonitrile (9.0 mL), and the mixture heated at 90 °C for 19 h. The solvent was evaporated under reduced pressure, the residue dissolved in acetonitrile and purification by column chromatography carried out (activated alumina, eluent: acetonitrile). The obtained powder was dissolved in dichloromethane, followed by the addition of diethyl ether to precipitate the product. The powder was collected by filtration and dried under vacuum to yield a white solid (66.2 mg, Yield 74%). $^1$H NMR (400 MHz, CD$_3$CN): δ = 0.93 (t, 3H, $J$ = 7.4 Hz, C$H_3$), 1.33–1.42 (m, 2H, C$H_2$CH$_3$), 1.51–1.59 (m, 2H, C$H_2$C$_2$H$_5$), 2.46 (t, 2H, $J$ = 8.0 Hz, C$H_2$C$_3$H$_7$), 5.28 (s, 5H, C$_5H_5$), 5.97–6.08 (m, 5H, Ar–$H_5$). IR (ATR, cm$^{-1}$): $\nu$ = 2926, 2855, 1457, 1418, 821, 726, 557. Anal. Calcd. for C$_{15}$H$_{19}$F$_6$PRu (445.35): C, 40.45; H, 4.30; N, 0.00. Found: C, 40.45; H, 4.25; N, 0.15.

**[1a][TFSA].** [**1a**][PF$_6$] (0.31 g, 0.69 mmol) was dissolved in a mixture of water and a small amount of acetone. An aqueous solution of Li[TFSA] (0.40 g, 0.39 mmol) was added to this solution, and the mixture stirred for 30 min. After the removal of acetone by evaporation, the resulting suspension was extracted with dichloromethane five times. The organic layer was dried over MgSO$_4$, and the solvent evaporated under reduced pressure. The residue was purified by column chromatography (activated alumina, eluent: dichloromethane and then ethanol–dichloromethane (5:95 v/v)). The resulting solution was evaporated under reduced pressure and the residue dried under vacuum at 80 °C for 17 h to give a colorless liquid (0.29 g, Yield 71%). $^1$H NMR (400 MHz, CD$_3$CN): δ = 0.93 (t, 3H, $J$ = 7.3 Hz, C$H_3$), 1.38 (sext, 2H, $J$ = 7.2 Hz, C$H_2$CH$_3$), 1.54 (quint, 2H, $J$ =

7.6 Hz, C$H_2$C$_2$H$_5$), 2.46 (t, 2H, $J$ = 7.6 Hz, C$H_2$C$_3$H$_7$), 5.27 (s, 5H, C$_5H_5$), 5.98–6.07 (m, 5H, Ar–$H_5$). IR (ATR, cm$^{-1}$): $\nu$ = 2961, 1526, 1458, 1417, 1348, 1331, 1178, 1132, 1051, 848, 738, 613, 599, 570. HRMS (ES$^+$) *m/z* calcd. for [C$_{15}$H$_{19}$Ru]$^+$: 301.0530. Found: 301.0530. Anal. Calcd. for C$_{17}$H$_{19}$F$_6$NO$_4$RuS$_2$ (580.52): C, 35.17; H, 3.30; N, 2.41. Found: C, 35.20; H, 3.26; N, 2.72.

**[1a][FSA].** Preparation as described for [**1a**][TFSA], using [**1a**][PF$_6$] (0.39 g, 0.88 mmol) and K[FSA] (0.49 g, 2.2 mmol). The desired product was obtained as a colorless liquid (0.24 g, Yield 57%). $^1$H NMR (400 MHz, CD$_3$CN): δ = 0.92 (t, 3H, $J$ = 7.2 Hz, C$H_3$), 1.37 (sext, 2H, $J$ = 7.2 Hz, C$H_2$CH$_3$), 1.54 (quint, 2H, $J$ = 7.6 Hz, C$H_2$C$_2$H$_5$), 2.46 (t, 2H, $J$ = 6.2 Hz, C$H_2$C$_3$H$_7$), 5.27 (s, 5H, C$_5H_5$), 6.01–6.07 (m, 5H, Ar–$H_5$). IR (ATR, cm$^{-1}$): $\nu$ = 1379, 1361, 1216, 1177, 1152, 1101, 823, 730, 567. HRMS (ES$^+$) *m/z* calcd. for [C$_{15}$H$_{19}$Ru]$^+$: 301.0530. Found: 301.0540. Anal. Calcd. for C$_{15}$H$_{19}$F$_2$NO$_4$RuS$_2$ (480.51): C, 37.49; H, 3.99; N, 2.91. Found: C, 37.28; H, 3.91; N, 2.91.

**Synthesis of [Ru(C$_5$H$_5$)(C$_6$H$_5$C$_8$H$_{17}$)][X] ([1b][X]; X = PF$_6$, TFSA, FSA)**

**[1b][PF$_6$].** Preparation as described for [**1a**][PF$_6$], using [Ru(C$_5$H$_5$)(NCCH$_3$)$_3$]PF$_6$ (0.18 g, 0.41 mmol), *n*-octylbenzene (0.17 g, 0.89 mmol), and acetonitrile (8.5 mL). Diethyl ether was added to a solution of the crude product in acetone, and the desired salt precipitated as a white solid (0.19 g, Yield 92%). $^1$H NMR (400 MHz, CD$_3$CN): δ = 0.88 (t, 3H, $J$ = 6.5 Hz, C$H_3$), 1.28 (m, 10H, (C$H_2$)$_5$CH$_3$), 1.56 (m, 2H, C$H_2$C$_6$H$_{13}$), 2.45 (t, 2H, $J$ = 1.4 Hz, C$H_2$C$_7$H$_{15}$), 5.27 (s, 5H, C$_5H_5$), 5.99–6.07 (m, 5H, Ar–$H_5$). IR (ATR, cm$^{-1}$): $\nu$ = 2926, 2855, 1467, 1457, 1418, 821, 726, 555. Anal. Calcd. for C$_{19}$H$_{27}$F$_6$PRu (501.46): C, 45.51; H, 5.43; N, 0.00. Found: C, 45.27; H, 5.35; N, 0.10.

**[1b][TFSA].** Preparation as described for [**1a**][TFSA], using [**1a**][PF$_6$] (0.18 g, 0.37 mmol) and Li[TFSA] (0.21 g, 0.73 mmol). The desired product was obtained as a pale yellow liquid (0.16 g, Yield 68%). $^1$H NMR (400 MHz, CD$_3$CN): δ = 0.88 (t, 3H, $J$ = 5.6 Hz, C$H_3$), 1.28 (m, 10H, (C$H_2$)$_5$CH$_3$), 1.56 (m, 2H, C$H_2$(C$_6$H$_{13}$), 2.45 (t, 2H, $J$ = 6.7 Hz, C$H_2$C$_7$H$_{15}$), 5.27 (s, 5H, C$_5H_5$), 5.98–6.06 (m, 5H, Ar–$H_5$). IR (ATR, cm$^{-1}$): $\nu$ = 1349, 1331, 1179, 1133, 1052, 849, 787, 739, 653, 614,

599, 570, 562. HRMS ($ES^+$) *m/z* calcd. for $[C_{19}H_{27}Ru]^+$: 357.1156. Found: 357.1162. Anal. Calcd. for $C_{21}H_{27}F_6NO_4RuS_2$ (636.63): C, 39.62; H, 4.28; N, 2.20. Found: C, 39.82; H, 4.05; N, 2.45.

**[1b][FSA].** Preparation as described for [**1a**][TFSA], using [**1b**][$PF_6$] (0.19 g, 0.39 mmol) and K[FSA] (0.17 g, 0.78 mmol). The desired product was obtained as a colorless solid (0.16 g, Yield 80%). $^1$H NMR (400 MHz, $CD_3CN$): δ = 0.88 (t, 3H, *J* = 5.6 Hz, C*H*$_3$), 1.29 (m, 10H, (C*H*$_2$)$_5$CH$_3$), 1.56 (m, 2H, C*H*$_2$C$_6$H$_{13}$), 2.45 (t, 2H, *J* = 7.8 Hz, C$_7$H$_{15}$), 5.27 (s, 5H, C$_5$*H*$_5$), 5.98–6.08 (m, 5H, Ar–*H*$_5$). IR (ATR, $cm^{-1}$): $\nu$ = 1379, 1361, 1178, 1101, 823, 774, 567. HRMS ($ES^+$) *m/z* calcd. for $[C_{19}H_{27}Ru]^+$: 357.1156. Found: 357.1161. Anal. Calcd. for $C_{19}H_{27}F_2NO_4RuS_2$ (536.61): C, 42.56; H, 5.07; N, 2.52. Found: C, 42.53; H, 5.07; N, 2.61.

**Synthesis of [Ru(C$_5$H$_5$)(C$_6$H$_5$OCH$_2$OCH$_3$)][X] ([2a][X]; X = PF$_6$, TFSA, FSA)**

**[2a][PF$_6$].** Preparation as described for [**1a**][$PF_6$], using [Ru(C$_5$H$_5$)(NCCH$_3$)$_3$]$PF_6$ (0.43 g, 1.0 mmol), (methoxymethoxy)benzene (0.28 g, 2.0 mmol), and acetonitrile (4.0 mL). Diethyl ether was added to a solution of the crude product in acetone, and the desired salt precipitated as a white solid (0.37 g, Yield 83%). $^1$H NMR (400 MHz, $CD_3CN$): δ = 3.40 (s, 3H, C*H*$_3$), 5.10 (s, 2H, C*H*$_2$OCH$_3$), 5.31 (s, 5H, C$_5$*H*$_5$), 5.87 (t, 1H, *J* = 5.6 Hz, Ar–*H*), 6.04 (t, 2H, *J* = 6.4 Hz, Ar–*H*$_2$), 6.19 (d, 2H, *J* = 6.4 Hz, Ar–*H*$_2$). IR (ATR, $cm^{-1}$) $\nu$ = 1526, 1458, 1244, 1153, 1089, 953, 819, 668, 555. Anal. Calcd. for $C_{13}H_{15}F_6O_2PRu$ (449.30): C, 34.75; H, 3.37; N, 0.00. Found: C, 34.86; H, 3.41; N, 0.17.

**[2a][TFSA].** Preparation as described for [**1a**][TFSA], using [**2a**][$PF_6$] (0.16 g, 0.36 mmol) and Li[TFSA] (0.21 g, 0.71 mmol). The desired product was obtained as a pale yellow liquid (0.19 g, Yield 90%). $^1$H NMR (500 MHz, $CD_3Cl$): δ = 3.52 (s, 3H, C*H*$_3$), 5.13 (s, 2H, C*H*$_2$OCH$_3$), 5.39 (s, 5H, C$_5$*H*$_5$), 6.02 (t, 1H, *J* = 5.6 Hz, Ar–*H*), 6.17 (t, 2H, *J* = 6.5 Hz, Ar–*H*$_2$), 6.26 (d, 2H, *J* = 6.2 Hz, Ar–*H*$_2$). IR (ATR, $cm^{-1}$): $\nu$ = 1461, 1417, 1348, 1330, 1132, 1051, 945, 846, 786, 739, 612, 599, 570. Anal. Calcd. for $C_{15}H_{15}F_6NO_6RuS_2$ (584.47): C, 30.83; H, 2.59; N, 2.40. Found: C, 31.00; H, 2.30; N, 2.53.

**[2a][FSA].** Preparation as described for [**1a**][TFSA], using [**2a**][$PF_6$] (0.35 g, 0.79 mmol) and K[FSA] (0.34 g, 1.57 mmol). This salt was a liquid after vacuum drying, but it solidified as a colorless solid when stored in a refrigerator (6 °C) overnight (0.29 g, Yield 76%). $^1$H NMR (400 MHz, $CD_3CN$): δ = 3.46 (s, 3H, C*H*$_3$), 5.11 (s, 2H, C*H*$_2$OCH$_3$), 5.30 (s, 5H, $C_5H_5$), 5.87 (t, 1H, *J* = 5.5 Hz, Ar–*H*), 6.03 (t, 2H, *J* = 6.5 Hz, Ar–*H*$_2$), 6.19 (d, 2H, *J* = 6.7 Hz, Ar–*H*$_2$). IR (ATR, cm$^{-1}$): $\nu$ = 1530, 1459, 1375, 1361, 1176, 1100, 959, 822, 736, 566. HRMS (ES$^+$) *m/z* calcd. for $[C_{13}H_{15}RuO_2]^+$: 305.0116. Found: 305.0116. Anal. Calcd. for $C_{13}H_{15}F_2NO_6RuS_2$ (448.45): C, 32.23; H, 3.12; N, 2.89. Found: C, 32.47; H, 3.04; N, 2.84.

**Synthesis of [Ru($C_5H_5$)($C_6H_5O(CH_2CH_2O)_2CH_3$)][X] ([2b][X]; X = $PF_6$, TFSA, FSA)**

**[2b][$PF_6$].** Preparation as described for [**1a**][$PF_6$], using [Ru($C_5H_5$)($NCCH_3$)$_3$]$PF_6$ (0.20 g, 0.46 mmol), 2-(2-methoxyethoxy)ethoxybenzene (0.18 g, 0.92 mmol), and acetonitrile (4.0 mL). Diethyl ether was added to a solution of the crude product in acetone, and the the desired product precipitated as a colorless solid (0.16 g, Yield 69%). $^1$H NMR (400 MHz, $CD_3CN$): δ = 3.29 (s, 3H, C*H*$_3$), 3.49 (m, 2H, C*H*$_2$OCH$_3$), 3.60 (m, 2H, C*H*$_2$CH$_2$OCH$_3$), 3.71 (m, 2H, C*H*$_2$OC$_2$H$_4$OCH$_3$), 4.05 (m, 2H, C*H*$_2$CH$_2$OC$_2$H$_4$OCH$_3$), 5.32 (s, 5H, $C_5H_5$), 5.85 (t, 1H, *J* = 5.5 Hz, Ar–*H*), 6.00 (t, 2H, *J* = 5.8 Hz, Ar–*H*$_2$), 6.13 (d, 2H, *J* = 6.4 Hz, Ar–*H*$_2$). IR (ATR, cm$^{-1}$): $\nu$ = 1530, 1446, 1416, 1256, 1242, 1136, 1101, 1063, 1039, 948, 821, 668, 555. Anal. Calcd. for $C_{16}H_{21}F_6O_3PRu$ (507.38): C, 37.88; H, 4.17; N, 0.00. Found: C, 37.86; H, 4.33; N, 0.29.

**[2b][TFSA].** Preparation as described for [**1a**][TFSA], using [**2b**][$PF_6$] (0.16 g, 0.32 mmol) and Li[TFSA] (0.18 g, 0.63 mmol). The desired product was obtained as a pale yellow liquid (0.18 g, Yield 90%). $^1$H NMR (500 MHz, $CD_3Cl$): δ = 3.38 (s, 3H, C*H*$_3$), 3.56–3.57 (m, 2H, C*H*$_2$OCH$_3$), 3.67–3.68 (m, 2H, C*H*$_2$CH$_2$OCH$_3$), 3.80 (t, 2H, *J* = 4.3 Hz, C*H*$_2$OC$_2$H$_4$OCH$_3$), 4.14 (t, 2H, *J* = 4.3 Hz, C*H*$_2$CH$_2$OC$_2$H$_4$OCH$_3$), 5.39 (s, 5H, $C_5H_5$), 5.91 (t, 1H, *J* = 5.6 Hz, Ar–*H*), 6.11 (t, 2H, *J* = 6.7 Hz, Ar–*H*$_2$), 6.24 (d, 2H, *J* = 6.2 Hz, Ar–*H*$_2$). IR (ATR, cm$^{-1}$): $\nu$ = 1530, 1463, 1417, 1349, 1331, 1179,

1132, 1051, 845, 787, 762, 739, 653, 613, 599, 570, 562. Anal. Calcd. for $C_{18}H_{21}F_6NO_7RuS_2$ (642.55): C, 33.65; H, 3.29; N, 2.18. Found: C, 33.72; H, 3.05; N, 2.25.

**[2b][FSA].** Preparation as described for [**1a**][TFSA], using [**2b**][$PF_6$] (0.052 g, 0.11 mmol) and K[FSA] (0.048 g, 0.22 mmol). The desired product was obtained as a colorless liquid (0.046 g, Yield 78%). $^1$H NMR (400 MHz, $CD_3CN$): δ = 3.29 (s, 3H, C*H*$_3$), 3.47–3.49 (m, 2H, C*H*$_2$OCH$_3$), 3.59–3.61 (m, 2H, C*H*$_2$CH$_2$OCH$_3$), 3.71 (t, 2H, *J* = 4.4 Hz, C*H*$_2$OC$_2$H$_4$OCH$_3$), 4.05 (t, 2H, *J* = 4.4 Hz, C*H*$_2$CH$_2$OC$_2$H$_4$OCH$_3$), 5.31 (s, 5H, C$_5$*H*$_5$), 5.85 (t, 1H, *J* = 5.7 Hz, Ar–*H*), 6.01 (t, 2H, *J* = 6.6 Hz, Ar–*H*$_2$), 6.13 (d, 2H, *J* = 6.6 Hz, Ar–*H*$_2$). IR (ATR, cm$^{-1}$): $\nu$ = 1529, 1462, 1417, 1379, 1361, 1258, 1216, 1178, 1141, 1101, 1060, 1038, 914, 824, 737, 666, 567. HRMS (ES$^+$) *m/z* calcd. for [$C_{16}H_{21}RuO_3$]$^+$: 363.0534. Found: 363.0536. Anal. Calcd. for $C_{16}H_{21}F_2NO_7RuS_2$ (542.53): C, 35.42; H, 3.90; N, 2.58. Found: C, 35.74; H, 3.95; N, 2.50.

**Synthesis of [Ru(C$_5$H$_5$)(C$_6$H$_5$OCH$_2$CH$_2$CH$_2$CN)][X] ([3a][X]; X = PF$_6$, TFSA, FSA)**

**[3a][PF$_6$].** Preparation as described for [**1a**][$PF_6$], using [Ru(C$_5$H$_5$)(NCCH$_3$)$_3$]$PF_6$ (0.10 g, 0.23 mmol), 4-phenoxybutyronitrile (74.0 mg, 0.46 mmol), and acetonitrile (1.0 mL). Ethyl acetate was added to solution of the crude product in acetone, the mixture sonicated, and the ethyl acetate layer removed by separation. This procedure was repeated ten times to remove unreacted ligand and resulted in precipitation of the salt as a white solid (80.0 mg, Yield 73%). $^1$H NMR (400 MHz, acetone-*d*$_6$): δ = 2.66 (m, 2H, C*H*$_2$CN), 2.81 (t, 2H, *J* = 5.6 Hz, C*H*$_2$CH$_2$CN), 4.12 (t, 2H, *J* = 5.6 Hz, C*H*$_2$C$_2$H$_4$CN), 5.41 (s, 5H, C$_5$*H*$_5$), 5.91 (t, 1H, *J* = 5.6 Hz, Ar–*H*), 6.01 (t, 2H, *J* = 6.2 Hz, Ar–*H*$_2$), 6.25 (d, 2H, *J* = 6.4 Hz, Ar–*H*$_2$). IR (ATR, cm$^{-1}$): $\nu$ = 2250, 1533, 1064, 1037, 823, 664, 555. Anal. Calcd for $C_{15}H_{16}F_6NOPRu$ (472.33): C, 38.14; H, 3.41; N, 2.97. Found: C, 38.15; H, 3.35; N, 3.19.

**[3a][TFSA].** Preparation as described for [**1a**][TFSA], using [**1a**][$PF_6$] (0.17 g, 0.35 mmol) and Li[TFSA] (0.20 g, 0.70 mmol). This salt was a liquid after vacuum drying but it solidified as a pale yellow solid when stored in a refrigerator (6 °C) overnight (0.11 g, Yield 51%). $^1$H NMR (400 MHz,

acetone-$d_6$): δ = 2.17 (t, 2H, $J$ = 5.8 Hz, C$H_2$CN), 2.71 (t, 2H, $J$ = 7.0 Hz, C$H_2$CH$_2$CN), 4.26 (t, 2H, $J$ = 5.8 Hz, C$H_2$C$_2$H$_4$CN), 5.56 (s, 5H, C$_5H_5$), 6.17 (t, 1H, $J$ = 5.6 Hz, Ar–$H$), 6.34 (t, 2H, $J$ = 6.4 Hz, Ar–$H_2$), 6.49 (d, 2H, $J$ = 6.4 Hz, Ar–$H_2$). IR (ATR, cm$^{-1}$): $\nu$ = 1530, 1455, 1352, 1335, 1260, 1176, 1134, 1048, 1008, 946, 846, 739, 609, 571, 561. Anal. Calcd. for $C_{17}H_{16}F_6N_2O_5RuS_2$ (607.50): C, 33.61; H, 2.65; N, 4.61. Found: C, 33.57; H, 2.43; N, 4.55.

**[3a][FSA].** Preparation as described for [**1a**][TFSA], using [**3a**][$PF_6$] (31.9 mg, 0.068 mmol) and K[FSA] (29.6 mg, 0.135 mmol). The desired product was obtained as a pale yellow liquid (38.2 mg, Yield 93%). $^1$H NMR (400 MHz, $CD_3CN$): δ = 2.04 (t, 2H, $J$ = 5.9 Hz, C$H_2$CN), 2.56 (t, 2H, $J$ = 7.0 Hz, C$H_2$CH$_2$CN), 3.99 (t, 2H, $J$ = 5.8 Hz, C$H_2$C$_2$H$_4$CN), 5.32 (s, 5H, C$_5H_5$), 5.86 (t, 1H, $J$ = 5.4 Hz, Ar–$H$), 6.02 (t, 2H, $J$ = 6.8 Hz, Ar–$H_2$), 6.11 (d, 2H, $J$ = 6.5 Hz, Ar–$H_2$). IR (ATR, cm$^{-1}$): $\nu$ = 2249, 1531, 1457, 1379, 1256, 1216, 1174, 1100, 1062, 1038, 1004, 947, 822, 722, 566. Anal. Calcd for $C_{15}H_{16}F_2N_2O_5RuS_2$ (507.49): C, 35.50; H, 3.18; N, 5.52. Found: C, 35.61; H, 2.88; N, 5.21.

**Synthesis of [Ru(C$_5$H$_5$)(C$_6$H$_5$O(CH$_2$)$_6$CN)][X] ([3b][X]; X = PF$_6$, TFSA, FSA)**

**[3b][PF$_6$].** Preparation as described for [**1a**][$PF_6$], using [Ru(C$_5$H$_5$)(NCCH$_3$)$_3$]$PF_6$ (0.20 g, 0.46 mmol), 7-phenoxyheptanenitrile (0.14 g, 0.67 mmol), and acetonitrile (2.0 mL). Toluene was added to a saturated solution of the crude product in acetone, the mixture sonicated, and the toluene layer removed by separation. This procedure was repeated ten times to remove unreacted ligand and resulted in precipitation of the salt as a white solid. The powder was collected by filtration, and this procedure was further repeated twice (38.6 mg, Yield 16%). $^1$H NMR (400 MHz, acetone-$d_6$): δ = 1.52 (m, 4H, (C$H_2$)$_2$CN), 1.68 (m, 2H, C$H_2$C$_2$H$_4$CN), 1.81 (m, 2H, C$H_2$C$_3$H$_6$CN), 2.49 (t, 2H, $J$ = 7.0 Hz, C$H_2$C$_4$H$_8$CN), 4.13 (t, 2H, $J$ = 6.4 Hz, C$H_2$C$_5$H$_{10}$CN), 5.51 (s, 5H, C$_5H_5$), 6.11 (t, 1H, $J$ = 5.6 Hz, Ar–$H$), 6.28 (t, 2H, $J$ = 6.2 Hz, Ar–$H_2$), 6.42 (d, 2H, $J$ = 6.8 Hz, Ar–$H_2$). IR (ATR, cm$^{-1}$): $\nu$ = 2251, 1530, 1460, 1258, 1011, 976, 822, 667, 555. Anal. Calcd. for $C_{18}H_{22}F_6NOPRu$ (514.41): C, 42.03; H, 4.31; N, 2.72. Found: C, 42.30; H, 4.22; N, 3.10.

**[3b][TFSA].** Preparation as described for [**1a**][TFSA], using [**3b**][$PF_6$] (39.0 mg, 0.075 mmol) and Li[TFSA] (43.0 mg, 0.15 mmol). The desired product was obtained as a pale yellow liquid (37.1 mg, Yield 76%). $^1$H NMR (400 MHz, acetone-$d_6$): δ = 1.54 (m, 4H, (C$H_2$)$_2$CN), 1.69 (m, 2H, C$H_2$C$_2$H$_4$CN), 1.83 (m, 2H, C$H_2$C$_3$H$_6$CN), 2.50 (t, 2H, $J$ = 7.3 Hz, C$H_2$C$_4$H$_8$CN), 4.15 (t, 2H, $J$ = 7.0 Hz, C$H_2$C$_5$H$_{10}$CN), 5.53 (s, 5H, C$_5H_5$), 6.14 (t, 1H, $J$ = 6.1 Hz, Ar–*H*), 6.32 (t, 2H, $J$ = 6.2 Hz, Ar–$H_2$), 6.45 (d, 2H, $J$ = 6.7 Hz, Ar–$H_2$). IR (ATR, cm$^{-1}$): $\nu$ = 1530, 1457, 1349, 1334, 1260, 1177, 1133, 1050, 1008, 845, 787, 738, 610, 570, 562. Anal. Calcd. for $C_{20}H_{22}F_6N_2O_5RuS_2$ (649.59): C, 36.98; H, 3.41; N, 4.31. Found: C, 36.87; H, 3.71; N, 4.02.

**[3b][FSA].** Preparation as described for [**1a**][TFSA], using [**3b**][$PF_6$] (17.2 mg, 0.033 mmol) and K[FSA] (14.6 mg, 0.067 mmol). The product was a liquid after vacuum drying but solidified as a pale yellow solid when stored in a refrigerator (6 °C) overnight (15.8 mg, Yield 86%). $^1$H NMR (400 MHz, $CD_3CN$): δ = 1.53 (m, 4H, (C$H_2$)$_2$CN), 1.68 (m, 2H, C$H_2$C$_2$H$_4$CN), 1.81 (m, 2H, C$H_2$C$_3$H$_6$CN), 2.49 (t, 2H, $J$ = 6.9 Hz, C$H_2$C$_4$H$_8$CN), 4.15 (t, 2H, $J$ = 6.3 Hz, C$H_2$C$_5$H$_{10}$CN), 5.53 (s, 5H, C$_5H_5$), 6.14 (t, 1H, $J$ = 5.8 Hz, Ar–*H*), 6.31 (t, 2H, $J$ = 6.8 Hz, Ar–$H_2$), 6.44 (d, 2H, $J$ = 6.5 Hz, Ar–$H_2$). IR (ATR, cm$^{-1}$): $\nu$ = 2250, 1531, 1458, 1380, 1363, 1258, 1178, 1103, 842, 821, 736, 722, 565. Anal. Calcd. for $C_{18}H_{22}F_2N_2O_5RuS_2$ (549.57): C, 39.34; H, 4.04; N, 5.10. Found: C, 39.64; H, 3.64; N, 4.80.

**Synthesis of [Ru(C$_5$H$_5$)(C$_6$H$_5$COCH$_2$CH$_2$CH$_3$)][X] ([4a][X]; X = PF$_6$, TFSA, FSA)**

**[4a][PF$_6$].** Preparation as described for [**1a**][$PF_6$], using [Ru(C$_5$H$_5$)(NCCH$_3$)$_3$]$PF_6$ (0.15 g, 0.35 mmol), butyrophenone (0.10 g, 0.69 mmol), and acetonitrile (1.0 mL). Diethyl ether was added to a solution of the crude product in dichloromethane, which was sonicated to precipitate the desired product as a white solid (0.12 g, Yield 77%). $^1$H NMR (400 MHz, $CD_3CN$): δ = 0.98 (t, 3H, $J$ = 7.5 Hz, C$H_3$), 1.65–1.76 (m, 2H, C$H_2$CH$_3$), 2.90 (t, 2H, $J$ = 7.2 Hz, C$H_2$C$_2$H$_5$), 5.35 (s, 5H, C$_5H_5$), 6.27 (m, 3H, Ar–$H_3$), 6.62–6.64 (m, 2H, Ar–$H_2$). IR (ATR, cm$^{-1}$) $\nu$ = 1741, 1702, 1406, 1374, 1204, 823,

753, 554. Anal. Calcd. for $C_{15}H_{17}F_6OPRu$ (459.33): C, 39.22; H, 3.73; N, 0.00. Found: C, 39.24; H, 3.92; N, 0.17.

**[4a][TFSA].** Preparation as described for [**1a**][TFSA], using [**4a**][$PF_6$] (0.17 g, 0.69 mmol) and Li[TFSA] (0.22 g, 0.76 mmol). The desired product was obtained as a pale yellow liquid (0.16 g, Yield 70%). $^1$H NMR (400 MHz, $CD_3CN$): δ = 0.98 (t, 3H, *J* = 7.5 Hz, C*H*$_3$), 1.70 (sext, 2H, *J* = 7.2 Hz, C*H*$_2$CH$_3$), 2.90 (t, 2H, *J* = 7.0 Hz, C*H*$_2$C$_2$H$_5$), 5.36 (s, 5H, C$_5$*H*$_5$), 6.27–6.29 (m, 3H, Ar–*H*$_3$), 6.63–6.64 (m, 2H, Ar–*H*$_2$). IR (ATR, cm$^{-1}$): $\nu$ = 1704, 1347, 1330, 1177, 1132, 1051, 850, 786, 739, 613, 599, 570, 562. Anal. Calcd. for $C_{17}H_{17}F_6NO_5RuS_2$ (594.51): C, 34.35; H, 2.88; N, 2.36. Found: C, 34.52; H, 3.12; N, 2.40.

**[4a][FSA].** Preparation as described for [**1a**][TFSA], using [**4a**][$PF_6$] (50.0 mg, 0.11 mmol) and K[FSA] (48.1 mg, 0.22 mmol). The desired product was obtained as a pale yellow liquid (45.2 mg, Yield 78%). $^1$H NMR (400 MHz, $CD_3CN$): δ = 0.98 (t, 3H, *J* = 7.4 Hz, C*H*$_3$), 1.70 (sext, 2H, *J* = 7.2 Hz, C*H*$_2$CH$_3$), 2.90 (t, 2H, *J* = 7.1 Hz, C*H*$_2$C$_2$H$_5$), 5.36 (s, 5H, C$_5$*H*$_5$), 6.27 (t, 3H, *J* = 4.9 Hz, Ar–*H*$_3$), 6.64 (m, 2H, *J* = 5.8 Hz, Ar–*H*$_2$). IR (ATR, cm$^{-1}$): $\nu$ = 1702, 1417, 1406, 1204, 819, 753, 555. Anal. Calcd. for $C_{15}H_{17}F_2NO_5RuS_2$ (494.49): C, 36.43; H, 3.47; N, 2.83. Found: C, 36.76; H, 3.41; N, 2.76.

**Synthesis of [Ru(C$_5$H$_5$)(C$_6$H$_5$CO(CH$_2$)$_6$CH$_3$)][X] ([4b][X]; X = PF$_6$, TFSA, FSA)**

**[4b][PF$_6$].** Preparation as described [**1a**][$PF_6$], using [Ru(C$_5$H$_5$)(NCCH$_3$)$_3$]$PF_6$ (0.11 g, 0.26 mmol), octanophenone (89.1 mg, 0.44 mmol), and acetonitrile (1.0 mL). Diethyl ether was added to a solution of the crude product in dichloromethane, and the mixture sonicated to precipitate the desired product. A hot dichloromethane solution of the product was treated with charcoal. After removal of charcoal by filtration, diethyl ether was added to the filtrate to precipitate the desired product, which was a white solid (96.1 mg, Yield 72%). $^1$H NMR (400 MHz, $CD_3CN$): δ = 0.87 (t, 3H, *J* = 7.0 Hz, C*H*$_3$), 1.29–1.35 (m, 10H, (C*H*$_2$)$_5$CH$_3$), 1.64 (t, 2H, *J* = 6.8 Hz, C*H*$_2$C$_5$H$_{10}$CH$_3$), 5.36 (d, 5H, C$_5$*H*$_5$), 6.15 (t, 3H, *J* = 7.0 Hz, Ar–*H*$_3$), 6.49–6.62 (m, 2H, Ar–*H*$_2$). IR (ATR, cm$^{-1}$): $\nu$ = 1703,

1418, 1191, 1089, 820, 703, 555. Anal. Calcd. for $C_{19}H_{25}F_6OPRu$ (515.44): C, 44.27; H, 4.89; N, 0.00. Found: C, 44.45; H, 4.65; N, 0.24.

**[4b][TFSA].** Preparation as described for [**1a**][TFSA], using [**4b**][$PF_6$] (0.15 g, 0.28 mmol) and Li[TFSA] (0.16 g, 0.57 mmol). The desired product was obtained as a pale yellow liquid (0.12 g, Yield 66%). $^1$H NMR (400 MHz, $CDCl_3$): δ = 0.88 (t, 3H, *J* = 7.0 Hz, C*H*$_3$), 1.29–1.34 (m, 8H, (C*H*$_2$)$_4$C$_2$H$_5$), 1.71 (t, 2H, *J* = 7.2 Hz, C*H*$_2$CH$_3$), 2.94 (t, 2H, *J* = 7.2 Hz, C*H*$_2$C$_6$H$_{13}$), 5.44 (s, 5H, C$_5$*H*$_5$), 6.40 (t, 1H, *J* = 5.6 Hz, Ar–*H*), 6.45 (t, 3H, *J* = 6.1 Hz, Ar–*H*$_2$), 6.79 (d, 2H, *J* = 6.1 Hz, Ar–*H*$_2$). IR (ATR, cm$^{-1}$): $\nu$ = 1701, 1349, 1332, 1179, 1137, 1048, 1008, 863, 788, 740, 610, 574, 562. Anal. Calcd. for $C_{21}H_{25}F_6NO_5RuS_2$ (650.61): C, 38.77; H, 3.87; N, 2.15. Found: C, 38.76; H, 3.70; N, 2.19.

**[4b][FSA].** Preparation as described for [**1a**][FSA], using [**4b**][$PF_6$] (96.1 mg, 0.19 mmol) and K[FSA] (81.7 mg, 0.37 mmol). The desired product was obtained as a pale yellow liquid (28.8 mg, Yield 28%). $^1$H NMR (400 MHz, $CD_3CN$): δ = 0.89 (t, 3H, *J* = 6.6 Hz, C*H*$_3$), 1.31–1.35 (m, 8H, (C*H*$_2$)$_4$C$_2$H$_5$), 1.64–1.69 (m, 2H, C*H*$_2$CH$_3$), 2.91 (t, 2H, *J* = 7.3 Hz, C*H*$_2$C$_6$H$_{13}$), 5.35 (s, 5H, C$_5$*H*$_5$), 6.15 (t, 3H, *J* = 4.5 Hz, Ar–*H*$_3$), 6.63 (d, 2H, *J* = 5.1 Hz, Ar–*H*$_2$). IR (ATR, cm$^{-1}$): $\nu$ = 1704, 1379, 1361, 1216, 1177, 1102, 1007, 824, 736, 567. Anal. Calcd. for $C_{19}H_{25}F_2NO_5RuS_2$ (550.60): C, 41.45; H, 4.58; N, 2.54. Found: C, 41.49; H, 4.61; N, 2.56.

## X-ray crystallography

Single crystals of [**1a**][$PF_6$], [**2a**][$PF_6$], [**2b**][$PF_6$], and [**4a**][$PF_6$] were grown by slow diffusion of diethyl ether into a concentrated dichloromethane solution of the salts. Single crystals of [**3a**][$PF_6$] were grown by vapor diffusion of diethyl ether into a concentrated dichloroethane solution. Single crystals of [**3b**][$PF_6$] were grown by slow cooling of an ethyl acetate solution. X-ray diffraction data were collected on a Bruker APEX II ULTRA CCD diffractometer using MoKα radiation ($\lambda$ = 0.71073 Å). All calculations were performed using SHELXTL[31]. Structures were solved by direct

methods (SHELXS 97) and expanded using Fourier techniques. All non-hydrogen atoms were refined anisotropically. Ortep 3 for Windows[32] was used to produce molecular graphics. Crystallographic parameters are listed in Table S1 in the ESI†. These data can be obtained free of charge from The Cambridge Crystallographic Data Centre via www.ccdc.cam.ac.uk/data_request/cif.


## Acknowledgements

This work was financially supported by KAKENHI (grant numbers 24350073 and 26104524). We thank Dr. Y. Furuie for elemental analyses and T. Ueda for his help with X-ray crystallography.


## References


1 (a) A. Stark and K. R. Seddon, in *Kirk-Othmer Encyclopedia of Chemical Technology*, Wiley-Interscience, New York, 5th edn, 2007, vol. 26, pp. 836–919. (b) *Ionic Liquids*: *Industrial Applications to Green Chemistry*, ed. R. D. Rongers and K. R. Seddon, ACS symposium series, American Chemical Sciety, Washington, D.C., 2002, vol. 818. (c) M. Armand, F. Endres, D. R. MacFarlane, H. Ohno, B. Scrosati, *Nat. Mater*. 2009, **8**, 621–629. (d) I. Krossing, J. M. Slattery, C. Daguenet, P. J. Dyson, A. Oleinikova, H. Weingärtner, *J. Am. Chem. Soc.* 2006, **128**, 3427–13434. (e) H. Weingärtner, *Angew. Chem., Int. Ed.* 2008, **47**, 654–670. (f) N. V. Plechkova and K. R. Seddon, *Chem. Soc. Rev.* 2008, **37**, 123–150.

2 (a) Y. Yoshida, G. Saito, in *Ionic Liquids: Theory, Properties, New Approaches*, ed. A. Kokorin, ISBN: 978-953-307-349-1, InTech, DOI: 10.5772/14846, 2011. (b) R. E. Del Sesto, C. Corley, A. Robertson, J. Wilkes, *J. Organomet. Chem.* 2005, **690**, 2536–2542. (c) A. Branco, L. C. Branco, F. Pina, *Chem. Commun.* 2011, **47**, 2300–2302. (d) P. Zhang, Y. Gong, Y. Lv, Y. Guo, Y. Wang, C. Wang, H. Li, *Chem. Commun.* 2012, **48**, 2334–2336. (e) P. Nockemann, B. Thijs, N. Postelmans, K. Van Hecke, L. Van Meervelt, K. Binnemans, *J. Am. Chem. Soc.* 2006, **128**, 13658–13659. (f) B. Mallick, B. Balke, C. Felser, A.-V. Mudring, *Angew. Chem., Int. Ed.*, 2008, **47**, 7635–7638. (g) Y.

Kohno, M. G. Cowan, M. Masuda, I. Bhowmick, M. P. Shores, D. L. Gin, R. D. Noble, *Chem. Commun.*, 2014, **50**, 6633-6636. (h) R. J. C. Brown, P. J. Dyson, D. J. Ellis, T. Welton, *Chem. Commun*., 2001, 1862–1863.

3 (a) H. Masui, R. W. Murray, *Inorg. Chem.* 1997, **36**, 5118–5126. (b) I. J. B. Lin, C. S. Vasam, *J. Organomet. Chem.* 2005, **690**, 3498–3512. (c) J. F. Huang, H. M. Luo, S. Dai, *J. Electrochem. Soc.* 2006, **153**, J9–J13. (d) M. Iida, C. Baba, M. Inoue, H. Yoshida, E. Taguchi, H. Furusho, *Chem. – Eur. J.* 2008, **14**, 5047–5056. (e) H. D. Pratt III, A. J. Rose, C. L. Staiger, D. Ingersoll, T. M. Anderson, *Dalton Trans*. 2011, **40**, 11396–11401. (f) N. R. Brooks, S. Schaltin, K. Van Hecke, L. Van Meervelt, K. Binnemans, J. Fransaer, *Chem.–Eur. J.* 2011, **17**, 5054–5059.

4 (a) Y. Funasako, T. Mochida, K. Takahashi, T. Sakurai, H. Ohta, *Chem.–Eur. J.* 2012, **18**, 11929–11936. (b) M. Okuhata, Y. Funasako, K. Takahashi, T. Mochida, *Chem. Commun.* 2013, **49**, 7662–7664. (c) Y. Funasako, M. Nosho, T. Mochida, *Dalton Trans.* 2013, **42**, 10138–10143. (d) Y. Miura, F. Shimizu, T. Mochida, *Inorg. Chem*. 2010, **49**, 10032–10040.

5 (a) T. Inagaki, T. Mochida, M. Takahashi, C. Kanadani, T. Saito, D. Kuwahara, *Chem.–Eur. J*. 2012, **18**, 6795–6804. (b) Y. Funasako, T. Mochida, T. Inagaki, T. Sakurai, H. Ohta, K. Furukawa, T. Nakamura, *Chem. Commun.* 2011, **47**, 4475–4477. (c) Y. Funasako, T. Inagaki, T. Mochida, T. Sakurai, H. Ohta, K. Furukawa, T. Nakamura, *Dalton Trans*. 2013, **42**, 8317–8327. (d) T. Inagaki and T. Mochida, *Chem.–Eur. J.*, 2012, **18**, 8070–8075. (e) S. Mori and T. Mochida, *Organometallics* 2013, **32**, 780–787. (f) T. Ueda and T. Mochida, *Organometallics*, DOI: 10.1021/acs.organomet.5b00021.

6 (a) F. C. Pigge and J. J. Coniglio, *Curr. Org. Chem.* 2001, **5**, 757–784. (b) T. P. Gill and K. R. Mann, *Organometallics* 1982, **1**, 485–488. (c) R. M. Moriarty, U. S. Gill, Y. Y. Ku, *J. Organomet. Chem.* 1988, **350**, 157–190.

7 S. Mori and T. Mochida, *Organometallics* 2013, **32**, 283–288.

8 S. Tang, G. A. Baker, H. Zhao, *Chem. Soc. Rev.* 2012, **41**, 4030–4066.

9 (a) Z. Zhou, H. Matsumoto, K. Tatsumi, *Chem. Eur. J.* 2005, **11**, 752–766. (b) Z. Zhou, H. Matsumoto, K. Tatsumi, *Chem. Eur. J.* 2004, **10**, 6581–6591.

10 Q. Zhang, Z. Li, S. Zhang, L. Zhu, J. Yang, X. Zhang, Y. Deng, *J. Phys. Chem. B* 2007, **111**, 2864–2872.

11 J. Leys, C. S. P. Tripathi, C. Glorieux, S. Zahn, B. Kirchner, S. Longuemart, K. C. Lethesh, P. Nockemann, W. Dehaen, K. Binnemans, *Phys. Chem. Chem. Phys.* 2014, **16**, 10548–10557.

12 (a) D. Turnbull and M. H. Cohen, *Modern Aspect of the Vitreous State*, Butterworth, London, 1960, Vol. **1**, p. 38. (b) O. Yamamuro, Y. Minamimoto, Y. Inamura, S. Hayashi, H. Hamaguchi, *Chem. Phys. Lett.* 2006, **423**, 371–375.

13 (a) D. R. MacFarlane and M. Forsyth, *Adv. Mater.* 2001, **13**, 957–966. (b) J. Timmermans, *J. Phys. Chem. Solids* 1961, **18**, 1–8.

14 H. Tokuda, K. Hayamizu, K. Ishii, Md. A. B. H. Susan, M. Watanabe, *J. Phys. Chem. B* 2004, **108**, 16593–16600.

15 (a) E. E. Karslyan, D. S. Perekalin, P. V. Petrovskii, K. A. Lyssenko, A. R. Kudinov, *Russ. Chem. Bull.* 2008, **57**, 2201–2203. (b) D. S. Perekalin, E. E. Karslyan, P. V. Petrovskii, A. O. Borissova, K. A. Lyssenko, A. R. Kudinov, *Eur. J. Inorg. Chem.* 2012, 1485–1492.

16 Q. Zhou, A. Henderson, G. B. Appetecchi, M. Montanino, S. Passerini, *J. Phys. Chem. B* 2008, **112**, 13577–13580.

17 K. Kubota, T. Nohira, R. Hagiwara, H. Matsumoto, *Chem. Lett.* 2010, **39**, 1303–1304.

18 H.-B. Han, S.-S. Zhou, D.-J. Zhang, S.-W. Feng, L.-F. Li, K. Liu, W.-F. Feng, J. Nie, H. Li, X.-J. Huang, M. Armand, Z.-B. Zhou, *J. Power. Sources.* 2011, **196**, 3623–3632.

19 a) H. Matsumoto, H. Sakaebe, K. Tatsumi, M. Kikuta, E. Ishiko, M. Kono, *J. Power Sources* 2006, **160**, 1308–1313. b) M. Ishikawa, T. Sugimoto, M. Kikuta, E. Ishiko, M. Kono, *J. Power Sources* 2006, **162**, 658–662. c) O. Borodin, W. Gorecki, G. D. Smith, M. Armand, *J. Phys. Chem. B* 2010, **114**, 6786–6798.

20 a) A. Paul and A. J. Samanta, *J. Phys. Chem. B* 2008, **112**, 16626–16632. b) H. Tokuda, K. Ishii, M. A. B. H. Susan, S. Tsuzuki, K. Hayamizu, M. Watanabe, *J. Phys. Chem. B*, **110**, 2833–2839 (2006).

21 G. S. Fulcher, *J. Am. Ceram. Soc.*, 1925, **8**, 339–355.

22 C. A. Angell, *J. Non-Cryst. Solids*, 1985, **73**, 1–17.

23 T. E. Youssef, M. M. El-Nahass, E. F. M. El-Zaidia, *J. Luminescence* 2013, **138**, 187–194.

24 J. Niziol, J. L. Fillaut, M. Sniechwski, F. Khammar, B. Sahraoui, *Opt. Mater.* 2012, **34**, 1670–1676.

25 C. Reichardt, *Green Chem*. 2005, **7**, 339–351.

26 J.-M. Lee, S. Ruckes, J. M. Prausnitz, *J. Phys. Chem. B* 2008, **112**, 1473–1476.

27 W. M. Reichert, J. D. Holbey, R. P. Swatloski, K. E. Gutowski, A. E. Visser, M. Nieuwenhuyzen, K. R. Seddon, R. D. Rogers, *Cryst. Growth Des*. 2007, **7**, 1106–1114.

28 (a) T. Mochida, Y. Funasako, M.-J. Li, T. Inagaki, D. Kuwahara, *Chem. Eur. J.* 2013, **19**, 6257–6264. (b) D. Braga and F. Grepioni, *Chem. Soc. Rev.* 2000, **29**, 229–238. (c) H. Schottenberger, K. Wurst, U. J. Griesser, R.K.R. Jetti, G. Laus, R. H. Herber, I. Nowik, *J. Am. Chem. Soc.* 2005, **127**, 6795–6801.

29 C. T. Vo, T. A. Mitchell, J. W. Bode, *J. Am. Chem. Soc.* 2011, **133**, 14082–14089.

30 J. W. Thackeray, S. M. Coley, V. Jain, O. Ongayi, J. F. Cameron, P. J. Labeaume, A. E. Madkour, *Eur. Pat. Appl.* 2012, 2472323.

31 (a) G. M. Scheldrick, *SHELXL: Program for the Solution for Crystal Structure*; University of Göttingen, Göttingen, Germany, 1997. (b) G. M. Sheldrick, *Acta Crystallogr*. 2008, **D64**, 112–122.

32 L. J. Farrugia, ORTEP-3 for Windows. *J. Appl. Crystallogr.* 1997, **30**, 565.

**Table of contents**

Colorless and stable metal-containing ionic liquids were prepared from cationic Ru(II) sandwich complexes, and their liquid properties were investigated in detail.

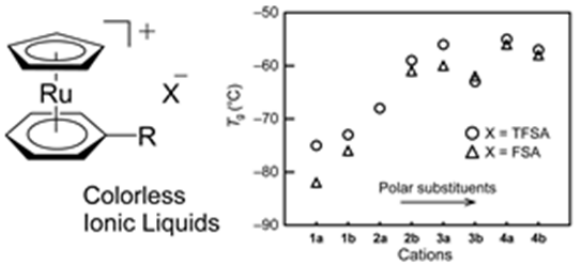

# Electronic supporting information

Colorless Organometallic Ionic Liquids from Cationic Ruthenium Sandwich Complexes: Thermal Properties, Liquid Properties, and Crystal Structures of $[Ru(\eta^5\text{-}C_5H_5)(\eta^6\text{-}C_6H_5R)][X]$ ($X = N(SO_2CF_3)_2$, $N(SO_2F)_2$, $PF_6$)

**Aina Komurasaki, Yusuke Funasako, Tomoyuki Mochida***

*Department of Chemistry, Graduate School of Science, Kobe University, Rokkodai, Nada, Hyogo 657-8501, Japan*

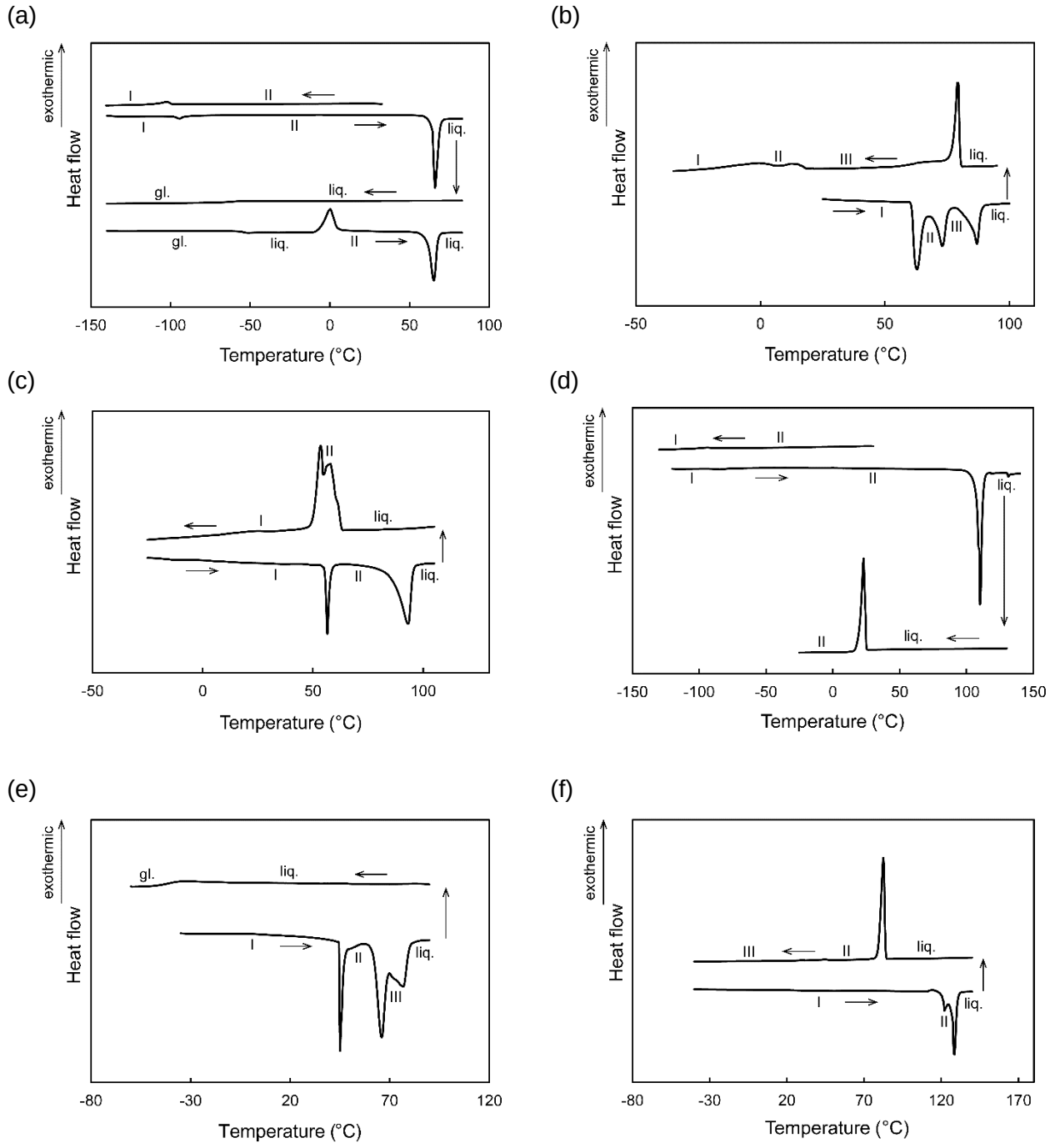


**Fig. S1.** DSC traces of (a) [**4a**][FSA], (b) [**1a**][$PF_6$], (c) [**1b**][$PF_6$], (d) [**2a**][$PF_6$], (e) [**2b**][$PF_6$], and (e) [**4a**][$PF_6$]. Glassy state and liquid phase are indicated as gl. and liq., respectively.

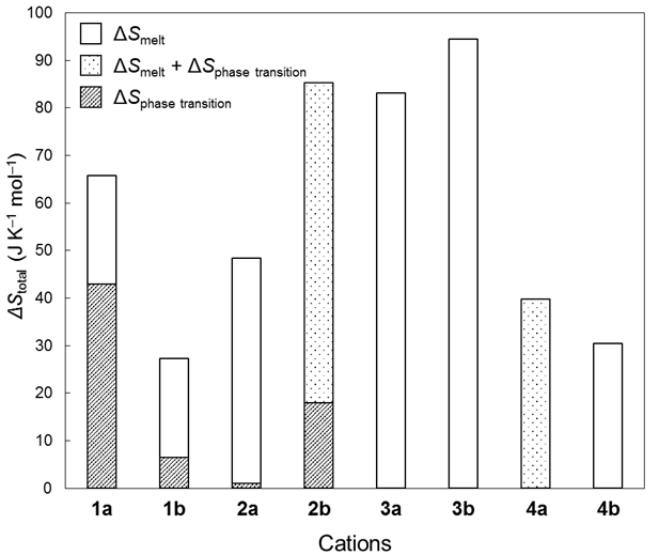


**Fig. S2.** Sum of the phase transition entropies of the $PF_6$ salts.

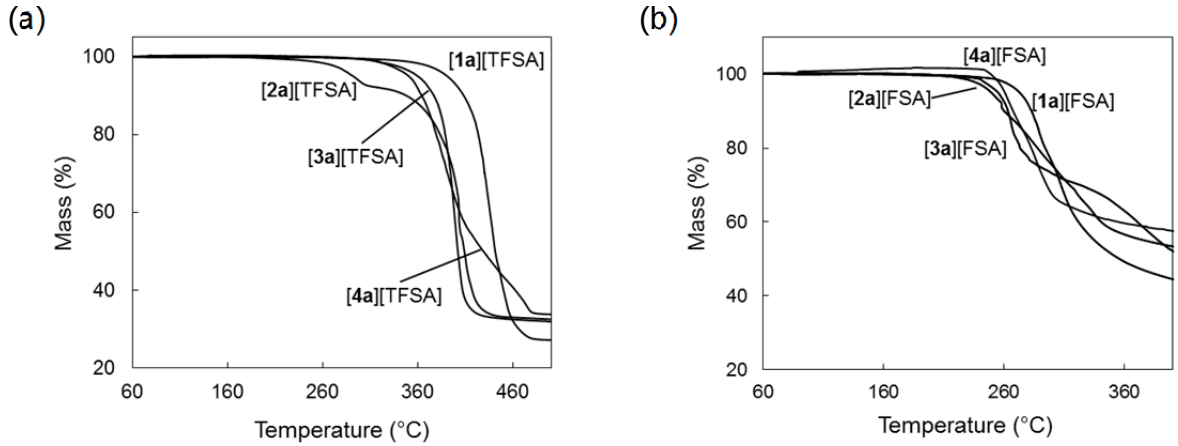


**Fig. S3.** Thermogravimetric traces of (a) [**1a**][TFSA]–[**4a**][TFSA] and (b) [**1a**][FSA]–[**4a**][FSA] (10 K $min^{-1}$).

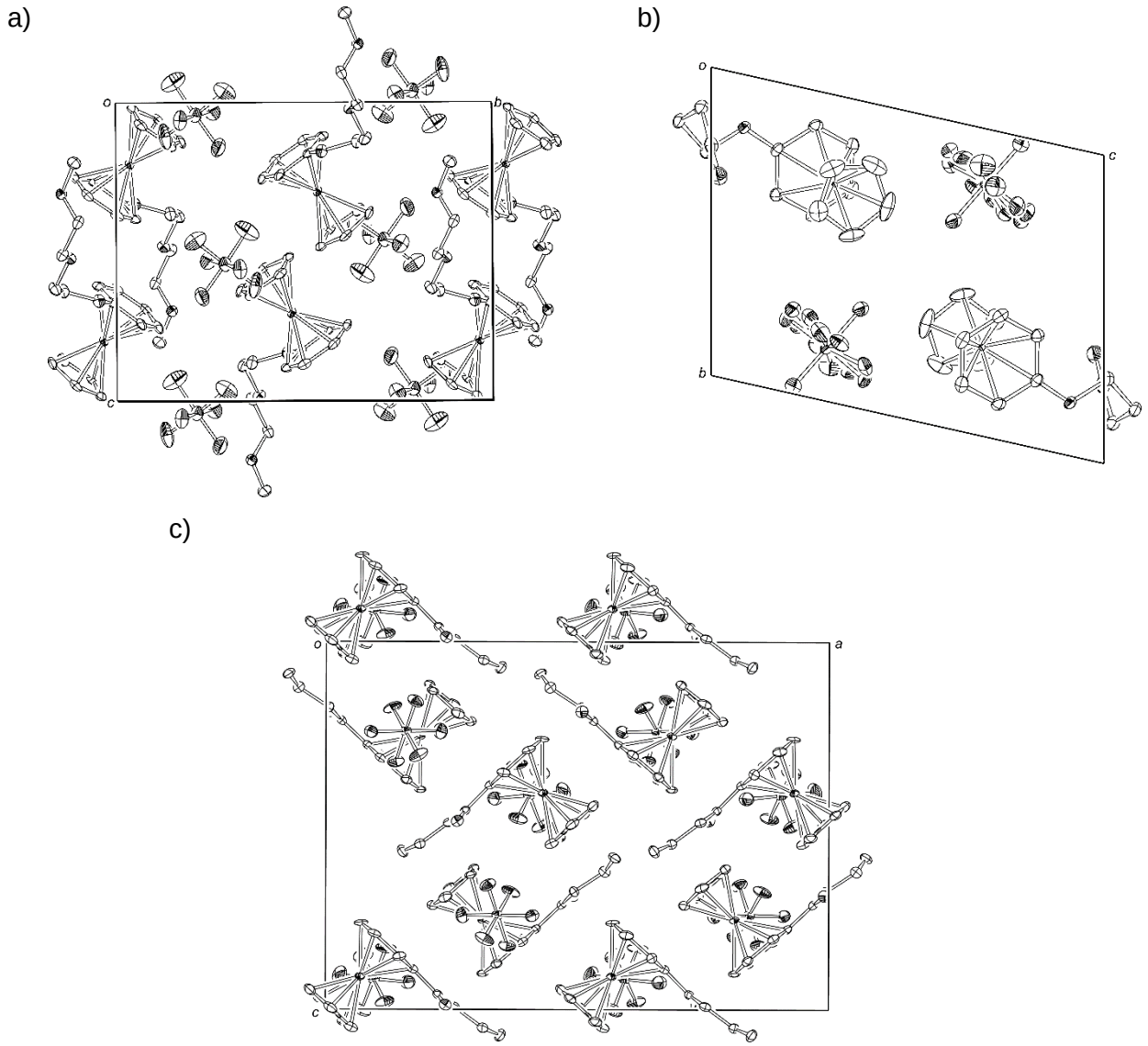


**Fig. S4.** Packing diagrams of (a) [**2b**][$PF_6$], (b) [**3a**][$PF_6$], and (c) [**4a**][$PF_6$].

**Table S1.** Crystallographic parameters.

| | [**1a**][$PF_6$] | [**2a**][$PF_6$] (100 K) | [**2a**][$PF_6$] (293 K) | [**2b**][$PF_6$] |
|---|---|---|---|---|
| Empirical formula | $C_{15}H_{19}F_6PRu$ | $C_{13}H_{15}F_6O_2PRu$ | | $C_{16}H_{21}F_6O_3PRu$ |
| Formula weight | 445.34 | 449.29 | | 507.37 |
| Crystal system | Monoclinic | Monoclinic | Orthorhombic | Monoclinic |
| Space group | *P* $2_1$/c | *P* $2_1$/c | *P* nma | *P* $2_1$/c |
| *a* (Å) | 7.6403(10) | 18.367(4) | 12.742(4) | 10.573(3) |
| *b* (Å) | 9.1602(12) | 8.8317(18) | 9.035(3) | 14.685(4) |
| *c* (Å) | 23.401(3) | 25.123(4) | 13.613(4) | 14.804(3) |
| *β* (°) | 108.800(4) | 133.146(10) | 90.0 | 128.135(12) |
| Volume (Å$^3$) | 1550.4(3) | 2973.4(10) | 1567.3(9) | 1807.9(8) |
| *Z* | 4 | 8 | 4 | 4 |
| $d_{calcd.}$ (g cm$^{-3}$) | 1.908 | 2.007 | 1.908 | 1.864 |
| *T* (K) | 100 | 100 | 293 | 100 |
| *μ* (mm$^{-1}$) | 1.172 | 1.233 | 1.17 | 1.03 |
| Reflections collected | 8011 | 14283 | 8253 | 8506 |
| Independent reflections | 3166 ($R_{int}$ = 0.0118) | 5246 ($R_{int}$ = 0.0742) | 1775 ($R_{int}$ = 0.0211) | 3193 ($R_{int}$ = 0.0204) |
| *F*(000) | 888 | 1776 | 888 | 1016 |
| $R_1$[a)], $wR_2$[b)] ($I > 2\sigma(I)$) | 0.0281, 0.0634 | 0.0286, 0.0741 | 0.0307, 0.0786 | 0.0421, 0.1110 |
| $R_1$[a)], $wR_2$[b)] (all data) | 0.0305, 0.0649 | 0.0292, 0.0752 | 0.0330, 0.0803 | 0.0440, 0.1128 |
| Goodness-of-fit on $F^2$ | 1.139 | 1.079 | 1.083 | 1.069 |
| Completeness to *θ* (%) | 99.5 | 99.7 | 99.8 | 99.8 |
| Parameters | 209 | 418 | 203 | 246 |
| Largest diff. peak and hole | 1.112 and –0.570 | 0.724 and –0.727 | 0.450 and –0.463 | 2.576 and 0.891 |

a) $R_1 = \Sigma \, ||F_o| - |F_c|| \, / \, \Sigma \, |F_o|$, b) $wR_2 = [\, \Sigma \, w(F_o^2 - F_c^2)^2 \, / \, \Sigma \, w(F_o^2)^2]^{1/2}$

(Continued)

| | [**3a**][$PF_6$] | [**3b**][$PF_6$] | [**4a**][$PF_6$] |
|---|---|---|---|
| Empirical formula | $C_{15}H_{16}F_6NOPRu$ | $C_{18}H_{22}F_6NOPRu$ | $C_{15}H_{17}F_6OPRu$ |
| Formula weight | 472.33 | 514.41 | 459.33 |
| Crystal system | Triclinic | Monoclinic | Orthorhombic |
| Space group | *P* –1 | *C* 2/c | *P* $ca2_1$ |
| *a* (Å) | 7.2737(14) | 9.871 (2) | 20.886(3) |
| *b* (Å) | 10.0402(19) | 19.268(5) | 10.4222(13) |
| *c* (Å) | 12.517(2) | 20.870(5) | 15.2449(19) |
| *β* (°) | 85.737(2) | 96.111 (4) | 90.0 |
| Volume ($Å^3$) | 845.8(3) | 2973.4(10) | 3318.5(7) |
| *Z* | 2 | 8 | 8 |
| $d_{calcd.}$ (g $cm^{-3}$) | 1.855 | 1.731 | 1.839 |
| *T* (K) | 100 | 100 | 100 |
| *μ* ($mm^{-1}$) | 1.086 | 0.939 | 1.103 |
| Reflections collected | 4167 | 8906 | 17705 |
| Independent reflections | 3013 ($R_{int}$ = 0.0137) | 3380 ($R_{int}$ = 0.0647) | 6457 ($R_{int}$ = 0.0579) |
| *F*(000) | 468 | 2064 | 1824 |
| $R_1$[a)], $wR_2$[b)] ($I > 2\sigma(I)$) | 0.0179, 0.0478 | 0.0414, 0.0930 | 0.0389, 0.1086 |
| $R_1$[a)], $wR_2$[b)] (all data) | 0.0183, 0.0481 | 0.0594, 0.1003 | 0.0411, 0.1111 |
| Goodness-of-fit on $F^2$ | 1.068 | 1.015 | 1.042 |
| Completeness to *θ* (%) | 97.6 | 97.0 | 100.0 |
| Parameters | 301 | 308 | 436 |
| Largest diff. peak and hole | 0.353 and –0.389 | 0.910 and –0.889 | 1.363 and –1.133 |

a) $R_1 = \Sigma \, ||F_o| - |F_c|| \, / \, \Sigma \, |F_o|$, b) $wR_2 = [\, \Sigma \, w(F_o^2 - F_c^2)^2 \, / \, \Sigma \, w(F_o^2)^2]^{1/2}$